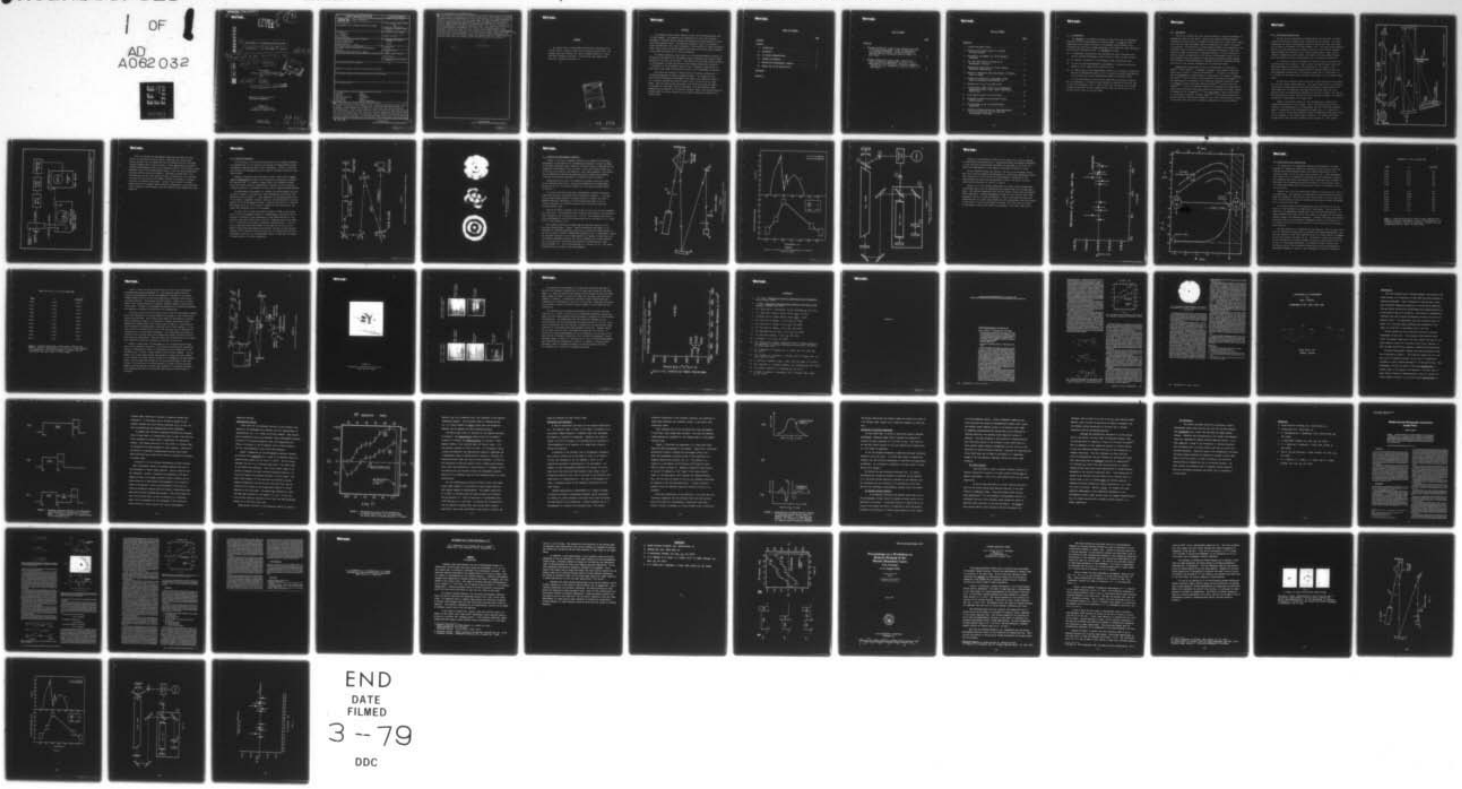
AD-A062 032 VERSAR INC SPRINGFIELD VA F/G 14/5
DEVELOPMENT OF AN INFRARED SCHLIEREN SYSTEM.(U)
OCT 78 T D WILKERSON, J M LINDSAY F44620-72-C-0076
UNCLASSIFIED 122-5 AFOSR-TR-78-1451 NL

1 OF 1
AD A062 032



END
DATE FILMED
3 -- 79
DDC

AFOSR-TR-78-1451

(18) (19)

Versar inc.

LEVEL II

(13)

AD A062032

DDC FILE COPY

(6) DEVELOPMENT OF AN INFRARED SCHLIEREN SYSTEM.

(10) T. D./Wilkerson, J. M./Lindsay and G. F./Frazier

(14) 122-5

(9) Final rept. 1 Jun 72-28 Feb 78,

(11) Oct 78 (12) 71 p.

DDC
DEC 11 1978
F

Final Report

Contract No. F44620-72-C-0076

(15)

(16) 2307 (17) A3

ORIGINAL CONTAINS COLOR PLATES: ALL DDC REPRODUCTIONS WILL BE IN BLACK AND WHITE.

Approved for public release;
distribution unlimited.

VERSAR INC.
6621 Electronic Drive
Springfield, Virginia 22151

October, 1978

389 335
78 12 04 130

SECURITY CLASSIFICATION OF THIS PAGE (When Data Entered)

REPORT DOCUMENTATION PAGE	READ INSTRUCTIONS BEFORE COMPLETING FORM
1. REPORT NUMBER **AFOSR-TR- 78-1451** 2. GOVT ACCESSION NO.	3. RECIPIENT'S CATALOG NUMBER
4. TITLE (and Subtitle) DEVELOPMENT OF AN INFRARED SCHLIEREN SYSTEM	5. TYPE OF REPORT & PERIOD COVERED FINAL 1 Jun 72 - 28 Feb 78
	6. PERFORMING ORG. REPORT NUMBER 122-5
7. AUTHOR(s) T D WILKERSON J M LINDSAY GENE F FRAZIER	8. CONTRACT OR GRANT NUMBER(s) F44620-72-C-0076
9. PERFORMING ORGANIZATION NAME AND ADDRESS VERSAR INCORPORATED 6621 ELECTRONIC DR SPRINGFIELD, VA 22151	10. PROGRAM ELEMENT, PROJECT, TASK AREA & WORK UNIT NUMBERS 2307A3 61102F
11. CONTROLLING OFFICE NAME AND ADDRESS AIR FORCE OFFICE OF SCIENTIFIC RESEARCH/NA BLDG 410 BOLLING AIR FORCE BASE, D C 20332	12. REPORT DATE Oct 78
	13. NUMBER OF PAGES 69
14. MONITORING AGENCY NAME & ADDRESS(if different from Controlling Office)	15. SECURITY CLASS. (of this report) UNCLASSIFIED
	15a. DECLASSIFICATION/DOWNGRADING SCHEDULE

16. DISTRIBUTION STATEMENT (of this Report)

Approved for public release; distribution unlimited.

17. DISTRIBUTION STATEMENT (of the abstract entered in Block 20, if different from Report)

18. SUPPLEMENTARY NOTES

19. KEY WORDS (Continue on reverse side if necessary and identify by block number)

SCHLIEREN	OZONE
INFRARED	ETHYLENE
LASER APPLICATIONS	PHOTOGRAPHY
BEAM PATTERN	IMAGING
REFRACTIVITY	FRINGE SEPARATION

20. ABSTRACT (Continue on reverse side if necessary and identify by block number)

The research covers several aspects of gas- and flow-visualization with infrared imagery. The purpose of the research was to show that infrared analogues of standard optical methods are suitable for visualizing flow fields containing molecular gases. The infrared refractive index $\underline{n}$ of molecular gases was measured at CO_2 laser frequencies. The variation of $\underline{n}$ near absorption lines forms a basis for species-selective schlieren (and other optical methods) having enhanced sensitivity to density gradients. Following preliminary tests using a x-y IR detector/scanner schlieren, we developed a new method of IR photography using conventional

DD FORM 1 JAN 73 1473

UNCLASSIFIED

SECURITY CLASSIFICATION OF THIS PAGE (When Data Entered)

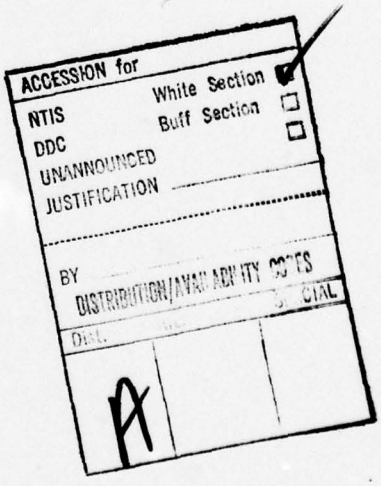
and Polaroid films designed for use with visible light. The result was a patented process suitable for photographic IR laser patterns and other images having power densities > /100 mw/cm^2 in the wavelength range 5-10 μm. Prospective applications to high energy laser beam profiling were disclosed to the Department of Defense. The method was applied to contract work on IR optics, principally to bi-prism measurements of gaseous refractive index. For comparison, high resolution interferometric measurements were made on the refractive index of air, nitrogen, ethylene and ozone at lines in the 9.6 and 10.6μ CO_2 laser bands. That the line-to-line variations of IR refractive index are indeed considerable in some gases, and are observable in an IR schlieren system, demonstrates the premise of the contract research, namely that species-selective methods based on optical refractivity are indeed suitable for improved flow visualization.

Sq. cm.

micrometers

FOREWORD

The authors wish to acknowledge the important contributions by the late Gene F. Frazier to many of the projects reported here. His untimely death has deprived the field of applied optics of a young and highly original contributor. We trust that this report does justice to the work he did with us.



78 12 04 170

Versar inc.

ABSTRACT

The research covers several aspects of gas- and flow-visualization with infrared imagery. The purpose of the research was to show that infrared analogues of standard optical methods are suitable for visualizing flow fields containing molecular gases. The infrared refractive index n of molecular gases was measured at CO_2 laser frequencies. The variation of n near absorption lines forms a basis for species-selective schlieren (and other optical methods) having enhanced sensitivity to density gradients.

Following preliminary tests using a x-y IR detector/scanner schlieren, we developed a new method of IR photography using conventional and Polaroid films designed for use with visible light. The result was a patented process suitable for photographic IR laser patterns and other images having power densities > /100 mw/cm^2 in the wavelength range 5-10 μm. Prospective applications to high energy laser beam profiling were disclosed to the Department of Defense.

The method was applied to contract work on IR optics, principally to bi-prism measurements of gaseous refractive index. For comparison, high resolution interferometric measurements were made on the refractive index of air, nitrogen, ethylene and ozone at lines in the 9.6 and 10.6μ CO_2 laser bands. That the line-to-line variations of IR refractive index are indeed considerable in some gases, and are observable in an IR schlieren system, demonstrates the premise of the contract research, namely that species-selective methods based on optical refractivity are indeed suitable for improved flow visualization.

Versar inc.

TABLE OF CONTENTS

		Page
FOREWARD		
ABSTRACT		
I.	INTRODUCTION	1
II.	BACKGROUND	2
III.	IR IMAGING DEMONSTRATIONS	3
IV.	INFRARED PHOTOGRAPHY	7
V.	REFRACTIVITY MEASUREMENTS (GENERAL)	10
VI.	RECENT WORK ON GAS REFRACTIVITY	17
REFERENCES		
APPENDIX A		

LIST OF TABLES

Page

Table No.

1 Standard refractivity (right column) computed from index of refraction measurements in C_2H_4 at approximately 0.015 atmosphere pressure. Extinction parameter α obtained from cell transmission $\exp(-\alpha\ell)$ where ℓ is path length 18

2 Standard refractivity (right column) computed from index of refraction measurements in O_3(3%) in O_2 at approximately 0.02 atmospheres. Extinction parameter α obtained from cell transmission, $\exp(-\alpha\ell)$, where ℓ is path length 19

LIST OF FIGURES

Figure No.		Page
1	Infrared Schlieren System	4
2	Detection and Display Method for Infrared Schlieren Scanner	5
3	Experimental Arrangement for IR Photographic Technique	8
4	CO_2 Laser Beam Patterns Recorded by IR Photographic Technique	9
5	Experimental System Used for Initial Gaseous Refractive Index Measure	11
6	Results of Refractive Index Measurements for Gaseous Ozone in Oxygen	12
7	Schematic of Refractivity Measurement System Using the Michelson Interferometer (C)	13
8	Refractivity of N_2 at CO_2 Laser Lines	15
9	Fringe Pattern (Upper Figure) and Corresponding Temperature Profile (Lower Figure) Approaching Heated Plate	16
10	Final Optical Layout for IR Schlieren	21
11	Photograph of Hollow Bi-Prism Used in Final Optical System	22
12	IR Photographs of the Bi-Prism/Schlieren Image Plane	23
13	Correlation between Refractive Index Measurements with Bi-Prism System and with Michelson Interferometer Techniques	25

I. Introduction

The purpose of the research has been to enlarge the body of techniques available for flow visualization in molecular gases. Our goal has been to demonstrate that infrared versions of the standard optical methods (e.g., schlieren) are effective in taking advantage of the refractive index variations near molecular absorption bands. The procedure has been:

(A) to demonstrate qualitatively that schlieren and other techniques work well at infrared wavelengths, using CO and CO_2 lasers as light sources,

(B) to develop a new method of IR photography using conventional film,

(C) to carry out wavelength-dependent measurements of molecular refractive index at low and high spectral resolution, and

(D) to conduct some of these measurements using both a schlieren configuration and the IR photographic method, so as to confirm the overall applicability of IR schlieren as a flow visualization method for molecular gases.

In this Final Report we will briefly summarize the previously reported work in categories 1-3 (above) and give details of research in the final year on topics in categories 3 and 4. Also we will call out specific R & D areas in which further work of use to AFOSR could be done, and which could not be pursued here for lack of time and funds.

II. Background

The use of schlieren and other optical methods to visualize phenomena in transparent fluids is well known. Optical path length differences between different ray paths are put in evidence by beam deflection or wave front retardation, and the resulting images require interpretation in terms of the index of refraction. The sensitivity of these methods depends on the magnitude of the refractive index, and can be enhanced by employing wavelengths at which the refractive index is maximized by anomalous dispersion. We have discussed in previous reports the magnitude of this effect for wavelength choices in the near infrared, where the presence of many molecular absorption bands implies the possibility of species-selective, enhanced sensitivity schlieren systems. This section lists related references for the interested reader.

Experimental and theoretical work on IR dispersion is discussed by Penner[1] and by Hadni[2]. Frequently, reviews of refractometer technology appear such as that by Leykin and Molochnikov[3]. The great care required even in measurements of simple gases is illustrated by the papers by Barrell and Sears[4,5] and the series of publications by Peck and his colleagues[6-10]. The consequences of the details of IR refraction and nearby absorption bands in atmospheric optics have been treated by Penndorf[11] and by Snider and Goldman[12]. The use of anomalous dispersion for enhanced flow visualization, using visible resonance lines, has recently been developed for plasma research by Koopman and his colleagues[13,14] following Koopman's early contributions to the present IR program. Numerous papers[15-18] have been published which are good guides to the overlap between IR laser lines and the molecular absorption spectra which give rise to anomalous dispersion in the near infrared.

Versar inc.

III. IR Imaging Demonstrations

Through 1974 we concentrated on demonstrating the usefulness of various classical visualization methods when transferred to the infrared. Schlieren, shadowgraph and shear interferometer pictures of heated gas flows were shown in our reports of December, 1973 and November, 1974. The light sources employed were CO, CO_2 and He-Ne lasers provided by Versar for this contract research. Image recording was carried out with liquid crystal sheets, "image plates" (based on desensitized fluorescence), pyroelectric detector/scanner systems, and a new method of direct IR photography that is discussed in Section IV.

It is useful to recall some aspects of the early work to facilitate discussions later in this report. Figure 1 shows the optical layout that, with minor modifications, remained in use during much of the research. This particular figure shows the schlieren field and imaging system (typical for many gasdynamic observations), the molecular laser, and — in this case — an x-y scanner for recording the IR intensity distribution in the schlieren image plane.

We used this scanning system to show that "point" detectors were compatible with the overall system operation. This was of some concern, to establish the broadest ultimate application of these techniques; in many cases low IR laser power will be necessary, requiring sensitive point detectors (e.g. Hg-Cd-Te) that are prohibitively expensive in the form of arrays. The success of this particular scanner implies that point-scanning in general is a feasible technique for experimental IR schlieren work.

Figure 2 illustrates the use of a CR oscilloscope in recording the intensity distribution in an IR image. The x-y CRO display copies the x-y location of the measurement in the laboratory, and the z (CRO beam intensity) control is governed by the instantaneous IR signal which is a function of x and y. Noise in the system is greatly reduced by matching an electronic filter to the frequency of the chopper shown in Figure 1. Of course, much faster systems can be used involving steerable optics instead of a slow scanner.

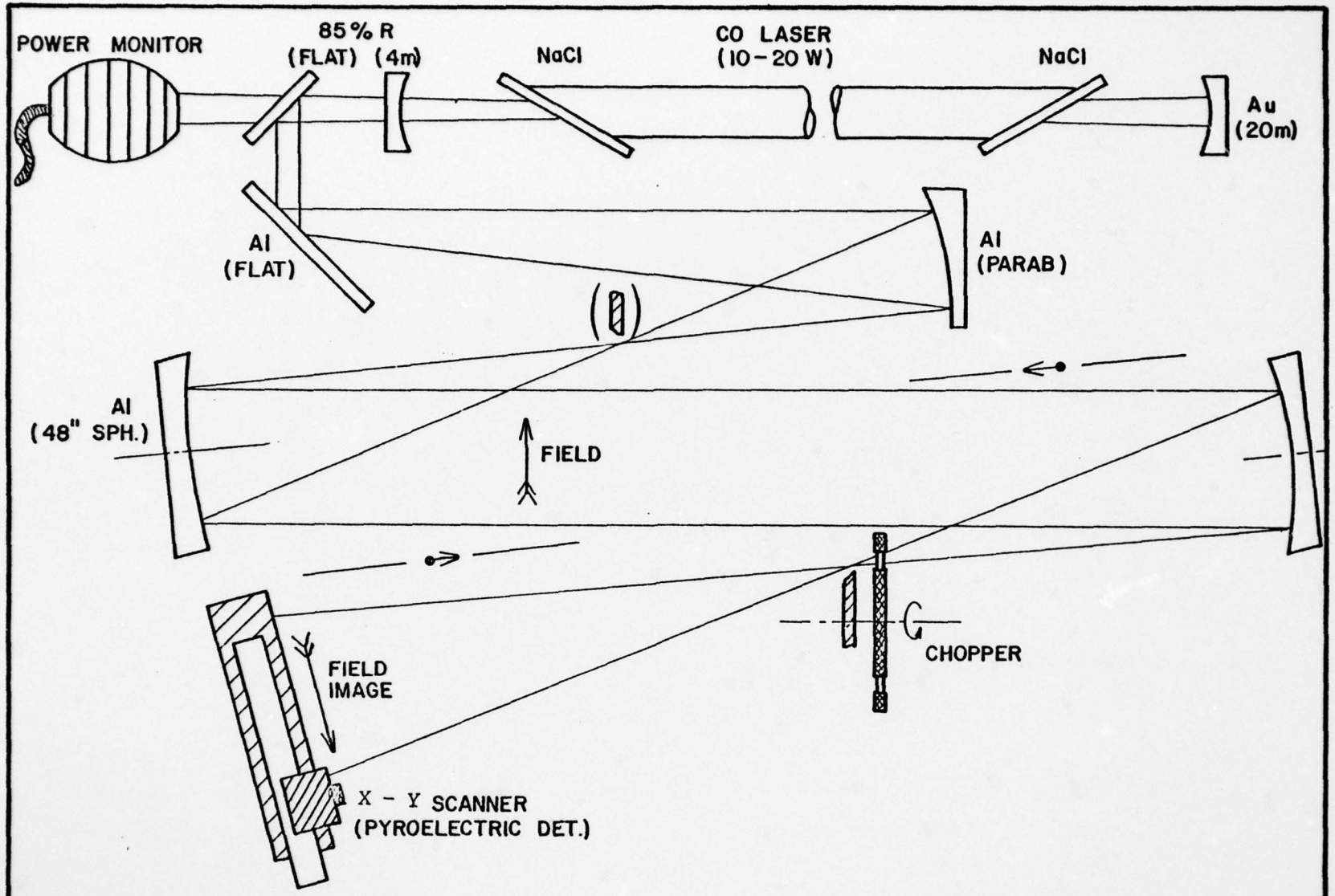


FIGURE 1 Infrared Schlieren System

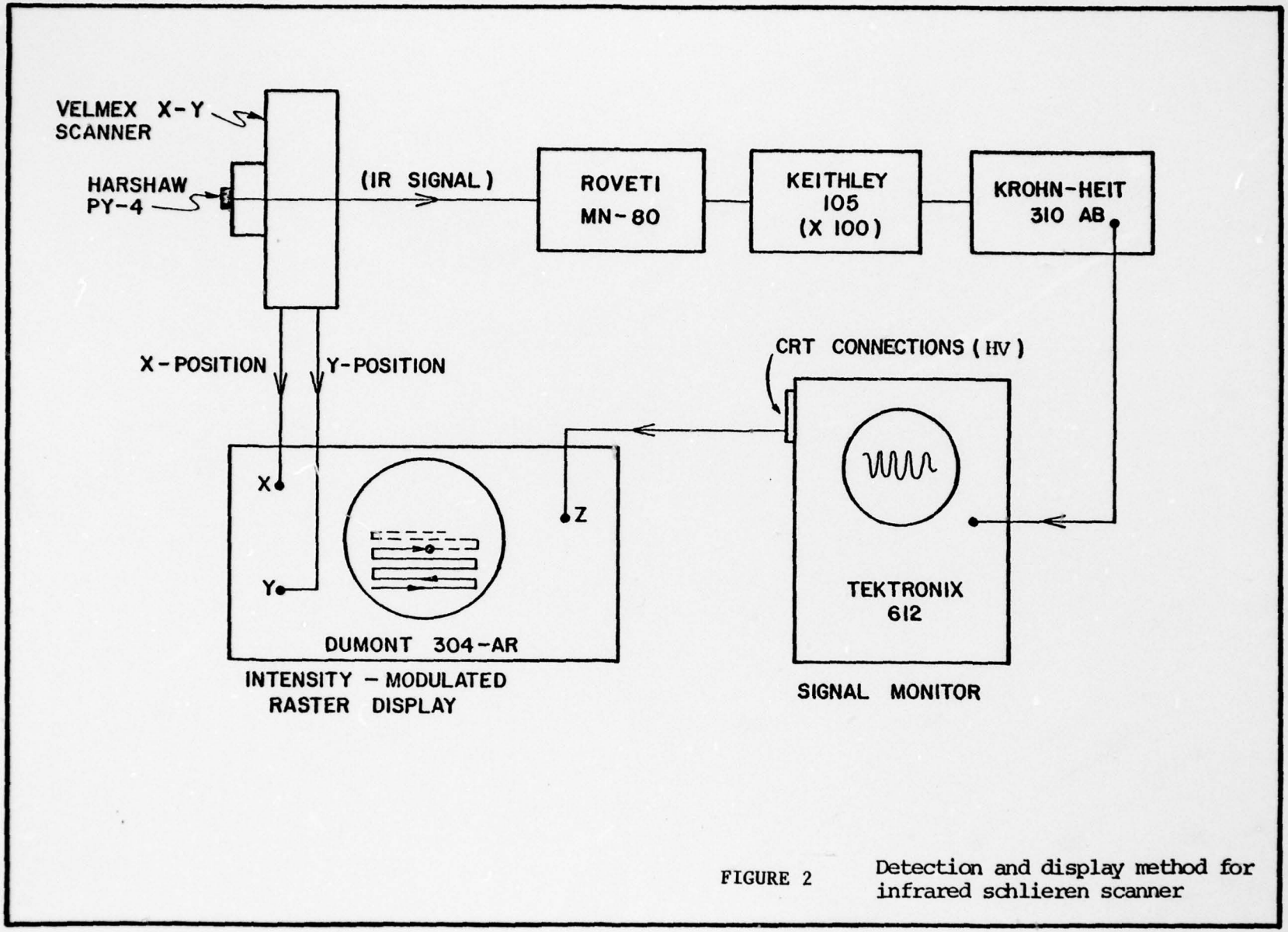


FIGURE 2 Detection and display method for infrared schlieren scanner

Versar inc.

Many IR schlieren and shadowgraph images were recorded with this system, as described in earlier reports, verifying that "white light" optical methods could be transferred into the infrared with the IR lasers running broadband with no line selection. These demonstrations included shearing interferograms taken in the integrated light of the CO_2 laser, using germanium flats as the interferometer plates. With this work accomplished, attention turned towards new methods of recording IR images and to the demonstration that the high resolution index of refraction (to be realized by single line operation of the lasers) afforded the prospect of species-selective IR schlieren photography. Section V also returns to another demonstration of IR imaging, where shearing interferometry was accomplished using a Michelson interferometer which was compatible with single-line laser operation.

Versar inc.

IV. Infrared Photography

In the course of our work involving the use of IR imaging techniques, we considered and put into practice the concept of desensitizing ordinary photographic emulsions by means of IR illumination. Indeed it was found that excellent IR photographs could be taken of schlieren fields and laser beam patterns.

Regimes of operation were discovered in which films could be sensitized or desensitized by means of IR illumination, depending on intensity and exposure time. In complex IR image fields, the boundaries between these two effects served as isophotometric contours for the IR pattern — a function difficult to accomplish by most other IR image-recording methods.

The experimental arrangement for studying the IR photographic process is shown in Figure 3, and three CO_2 laser beam patterns recorded by this method are shown in Figure 4. Other samples of the technique appear later in the report. Appendix A contains copies of five publications on various aspects of the IR photographic method. United States Patent No. 4,018,608 was granted April 19, 1977 to Gene F. Frazier for this new process, and rights were assigned to the U.S. Government.

In early 1976 a Concept Disclosure was made to AFOSR on the adaptation of the IR photographic method to cinematography, principally for the purpose of studying the time dependence of laser beam patterns for long duration, high power lasers such as the GDL. Exposure times in the range 1/10 - 1/100 second were useful at modest IR power densities. This concept is mentioned again here because of the ease and low cost of this method in providing beam imagery, particularly now that the "dry process" Polaroid film is available in movie film form. We believe that the cinematographic version of the IR photographic method is important to develop for applications to IR laser diagnostics.

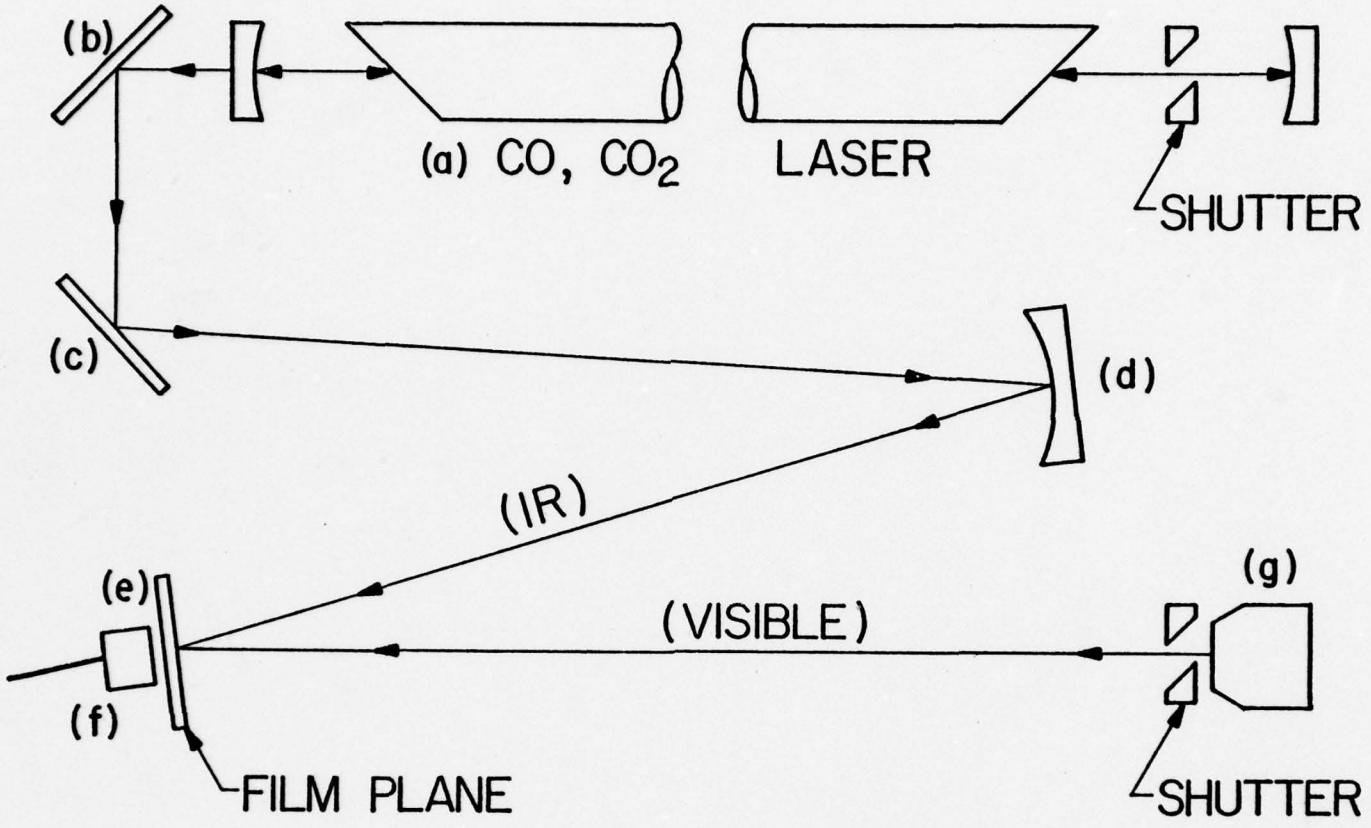


FIGURE 3

Experimental Arrangement for IR Photographic Technique



FIGURE 4

CO_2 Laser Beam Patterns Recorded by
IR Photographic Technique

Versar inc.

V. Refractivity Measurements (General)

Central to the use of anomalous dispersion for improved IR schlieren photography is the selection of illuminating wavelengths to match the edges of molecular absorption lines, where the refractive index is enhanced and the absorption by the medium is not too great. Since laser light sources (e.g., CO and CO_2) will often be used because of their high brightness, the problem can be redefined as finding the appropriate match between laser emission lines and the absorption spectrum of the molecular gas of interest.

Operationally this calls for measuring the gaseous refractive index at the available laser lines. This section summarizes such measurements made prior to 1977, and the more recent work is covered in greater detail in Section VI.

Our first (and lowest resolution) measurements of gaseous refractive index were made with the optical layout indicated in Figure 5. A two pass hollow prism (single chamber) containing the gas of interest was used to generate beam spot deflections at the schlieren knife edge, so as to indicate variations in refractive index as the IR laser was tuned over various emission lines.

Results are shown in Figure 6 for the gas O_3 (3%) in O_2 and for prominent CO_2 laser lines. The refractive index is seen to be greatest in the absorption notch longward of the ν_3 band of O_3 at ~ 9.6 μm. The estimated precision of index measurements by this hollow prism method was of the order of 2 to 3 parts in 10^6 in the quantity (n-1).

Much greater precision was sought via the classical approach of the Michelson interferometer. Figure 7 shows the Michelson instrument (C) we developed for infrared operation, along with an intracavity tuning etalon (A) for the CO_2 laser, intensity compensating detectors (B,E) to automatically adjust the perceived intensity in the fringe pattern for changes in laser power, and an intensity balancing polarizer (D) used to compensate for variable absorption in the gas cell. This system was capable of determining the laser line wavelength to ± .005 μm and measuring n to 1/10 part in 10^6. The interferometer optics are made of NaCl and germanium.

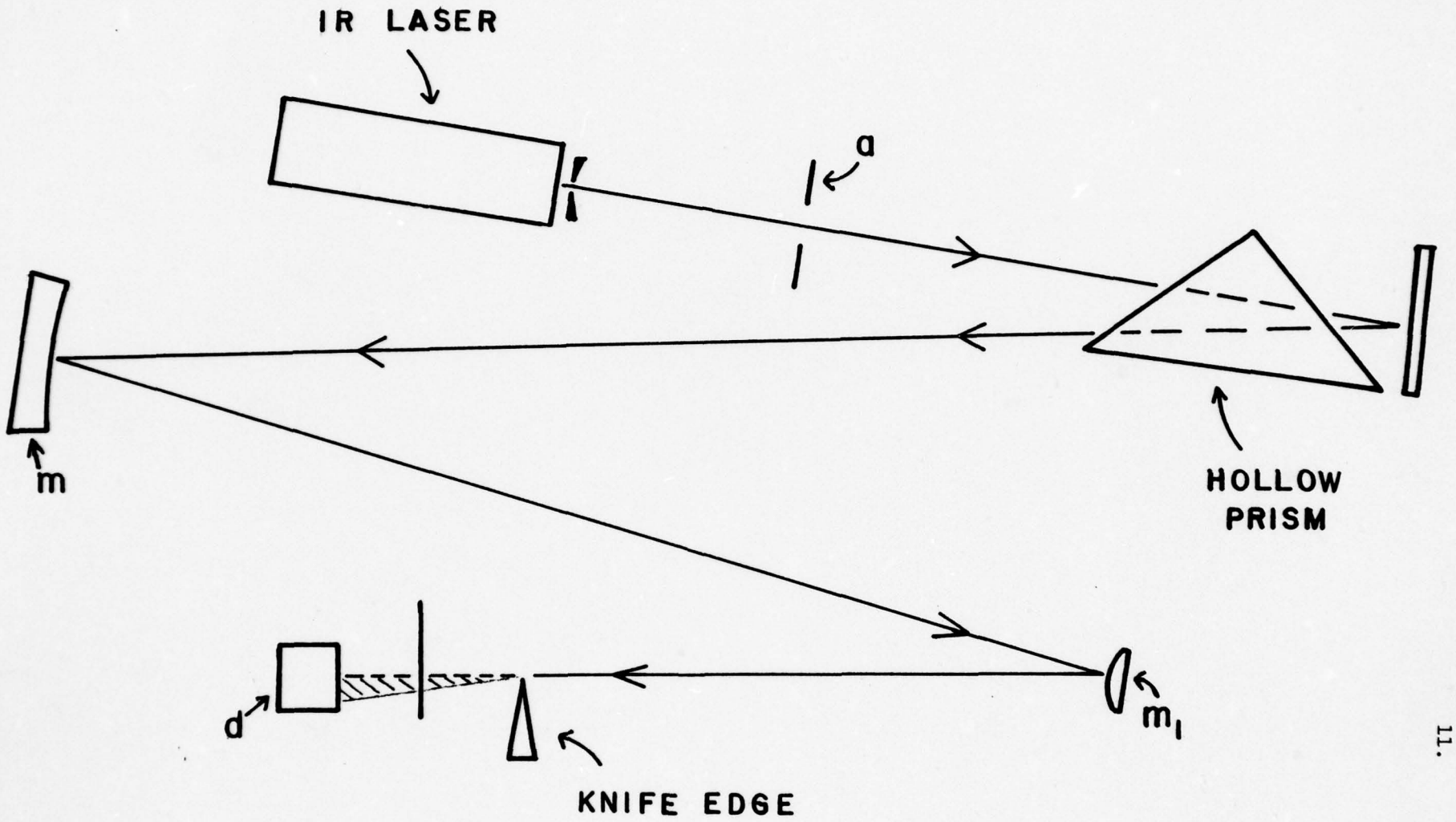


FIGURE 5

Experimental System Used for Initial Gaseous
Refractive Index Measure

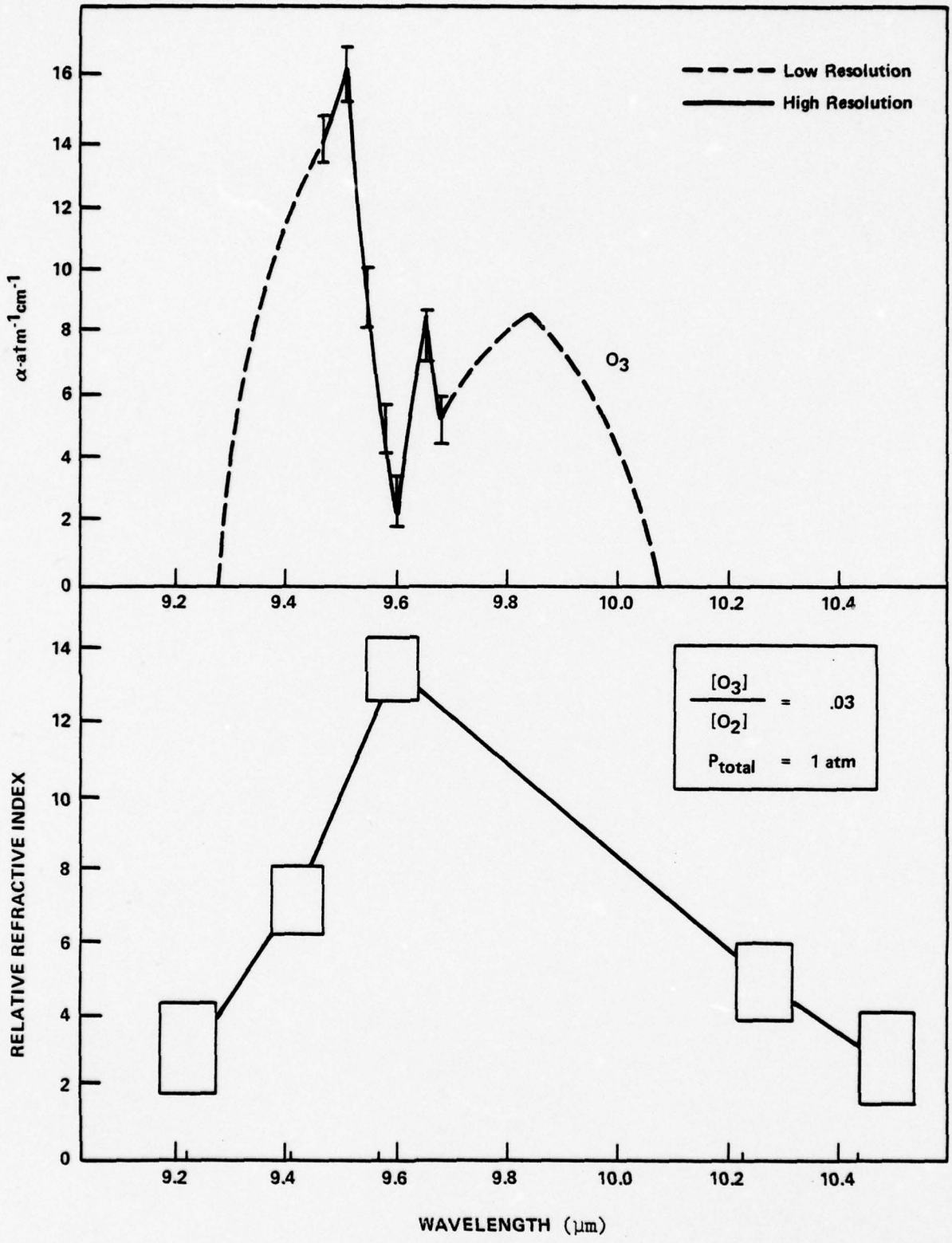


FIGURE 6

Results of Refractive Index Measurements for Gaseous Ozone in Oxygen

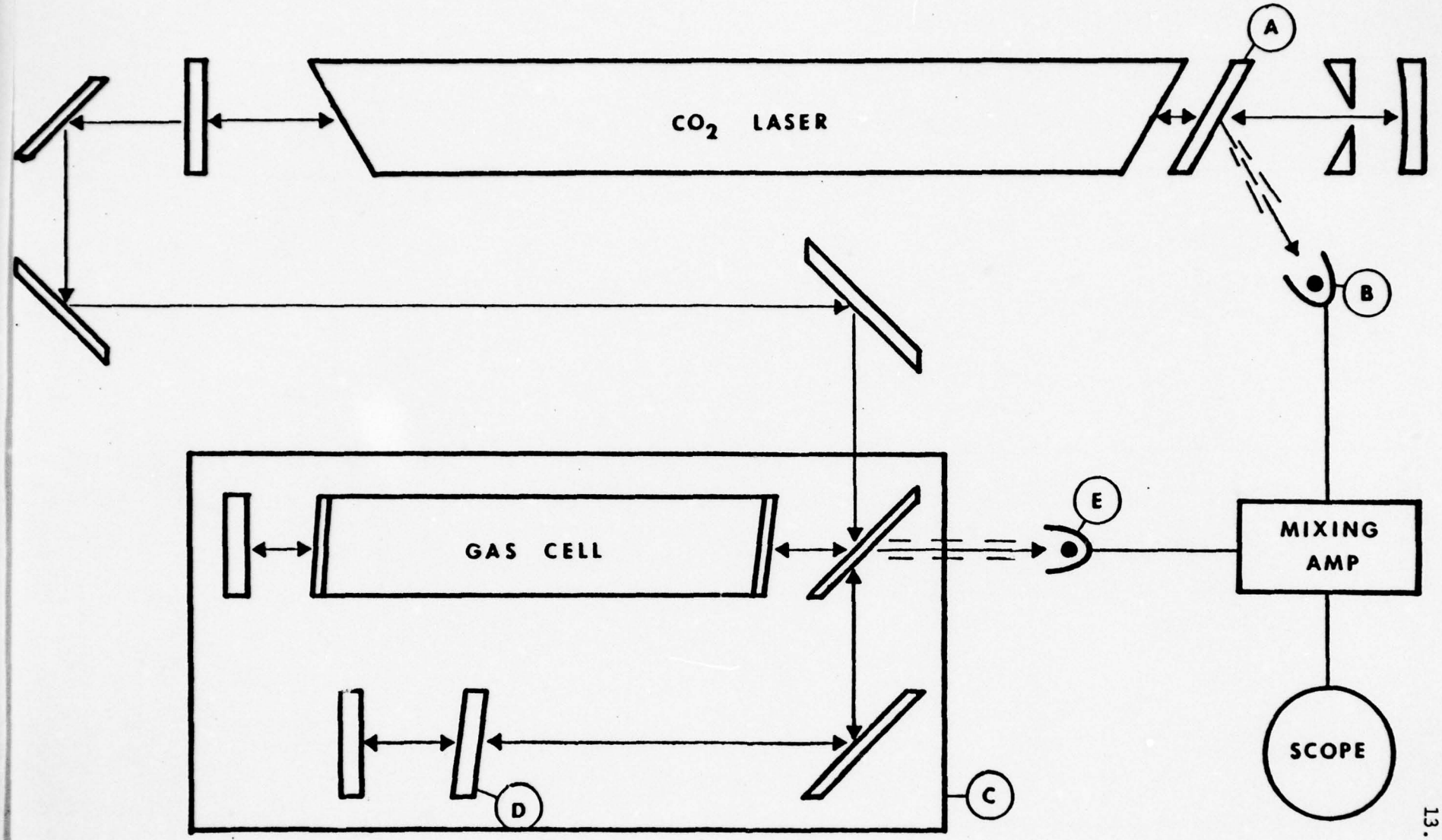


FIGURE 7

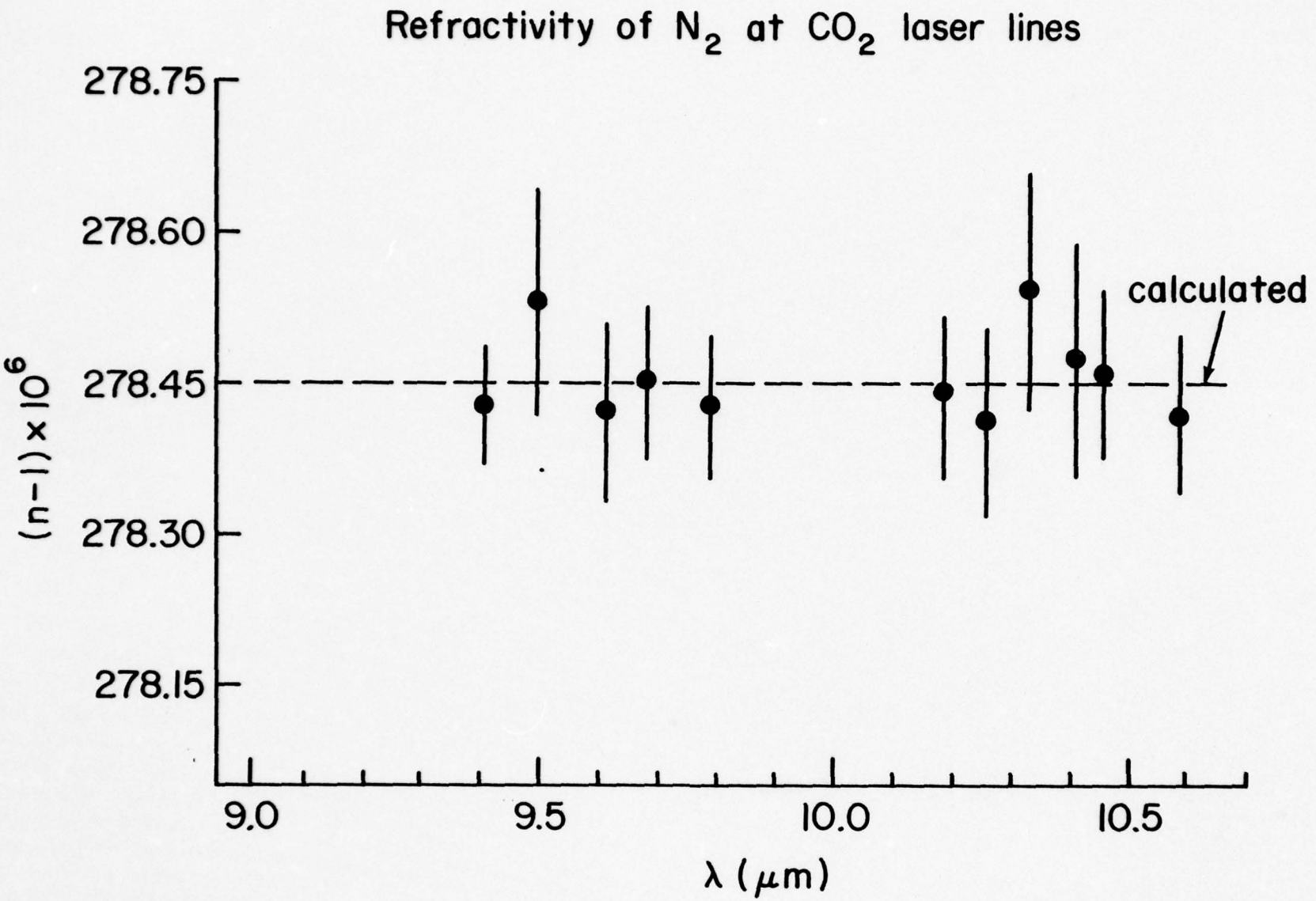
Schematic of Refractivity Measurement System
Using the Michelson Interferometer (C)

Results are illustrated by Figure 8 which shows our N_2 results compared to calculations from earlier work. Having established the expected performance of this relatively sophisticated instrument we proceeded to use it for refractivity measurements on other gases as described in Section VI below.

We also reported during this period on the use of the Michelson instrument as an infrared shearing interferometer for visualizing temperature-induced flow fields set up in one arm of the interferometer, illuminated by the line-selected CO_2 laser, and photographed by means of the direct IR photographic method discussed in Section IV (above).

Figure 9 is a line drawing representing the fringe pattern photographed as described above, and the temperature data reduced from the IR fringe photograph. The infrared temperature near the wall agrees closely with the measured plate temperature. Similar experiments carried out with a He-Ne laser showed comparable results at visible wavelengths. Thus we confirmed once again the transferability of visible light methods of flow visualization into the infrared at more than 10 times the wavelength, including, this time, both the direct IR photographic process and single-line operation of the laser light source.

FIGURE 8


Refractivity of N_2 at CO_2 laser lines
278.75
278.60
278.45
278.30
278.15
$(n-1) \times 10^6$
calculated
9.0
9.5
10.0
10.5
λ (μm)

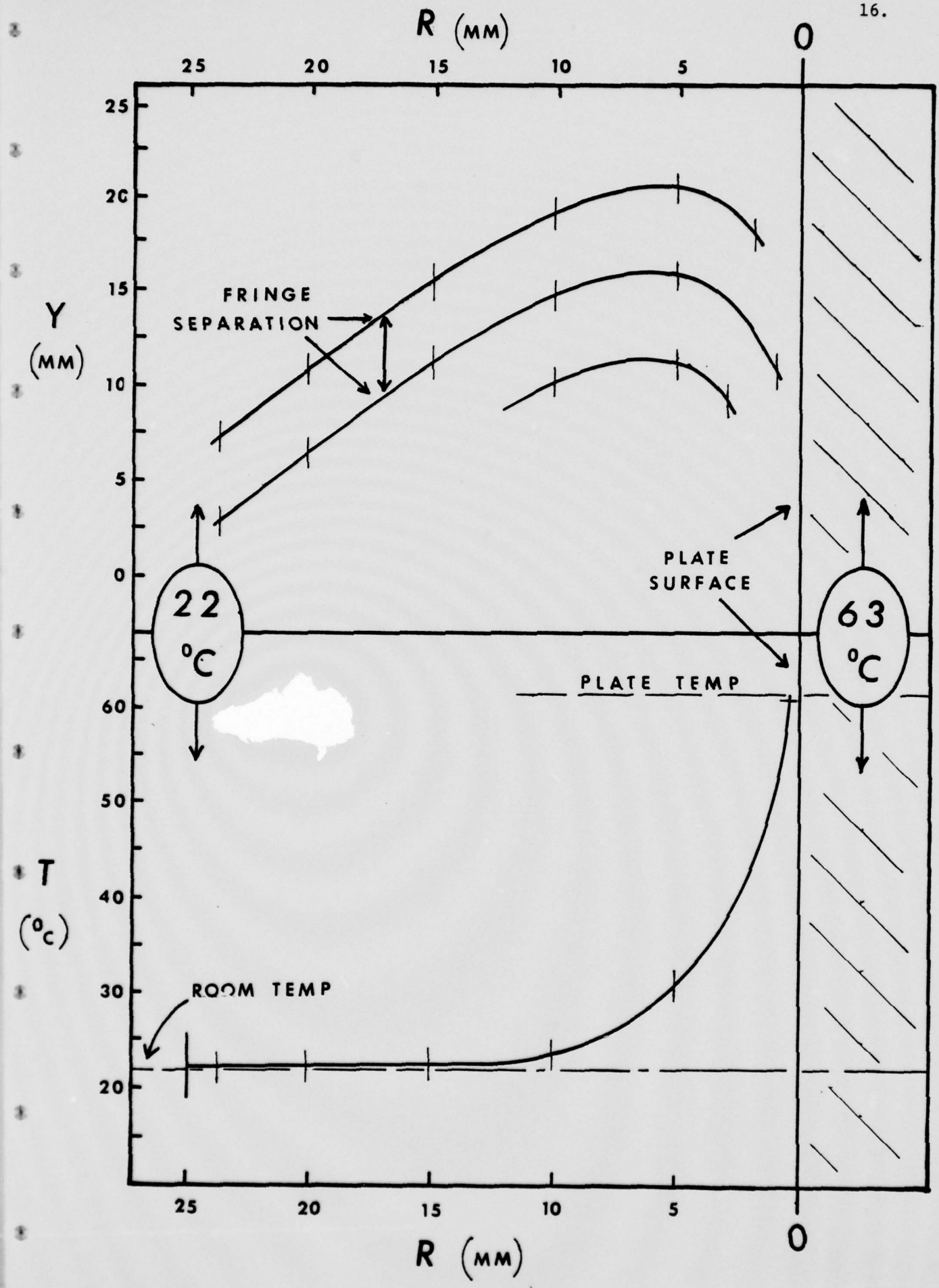


FIGURE 9

Fringe Pattern (Upper Figure) and Corresponding Temperature Profile (Lower Figure) Approaching Heated Plate

VI. Recent Work on Gas Refractivity

The perfection of a compensated Michelson interferometric technique enabled us to measure the refractive properties of gases such as ozone and ethylene which have absorption bands (and therefore excursions in the refractive index) in the CO_2 laser region around 10 μm. These measurements were carried out at low pressures and scaled into STP conditions, though it was recognized that actual high pressure (STP) conditions would increase the absorption line broadening and modify the details of the refractive index. The connection between high and low pressure results is discussed at the end of this section.

Tables 1 and 2 list the refractivity results for C_2H_4 and for O_3 (3%) in O_2 respectively. The variations in refraction are quite noticeable, particularly for ethylene at the R(20) and R(24) lines of the 9.6 μm CO_2 laser band. Also, the variations in ozone are impressive considering the small percentage of O_3 in the O_2 carrier gas.

It should be noted that the measurements were carried out in the presence of a wide variation in attenuation of these gases. This was possible because of the compensation systems built into the Michelson apparatus. We would recommend that future work of this kind be so designed for the maximum possible range of the important parameters. Enhanced refraction and absorption go hand in hand, so that absorption compensation needs to be allowed for at the outset, as well as the large variation in laser power over the molecular bands employed.

The next question to be addressed was the degree to which the high resolution $n(\lambda)$ behavior of gases could be inferred from simpler measurements — and how this behavior in turn would manifest itself in a simple optical arrangement such as the classical schlieren set up. We decided to answer both questions at once by means of a bi-prism technique, wherein one would directly test the ability of a knife edge measurement to distinguish between "optical path difference objects" that contained different gases and were illuminated at wavelengths designed to bring out the differences in refractive properties.

ETHYLENE, 9.6 μm CO_2 LASER BAND

line	α	$(n-1)\times10^6$
P(20)	0.41	377
P(18)	0.78	377
P(16)	0.72	389
P(14)	0.16	376
P(12)	0.13	378
P(10)	0.42	390
R(10)	0.33	385
R(12)	0.084	375
R(14)	0.076	375
R(16)	0.27	381
R(18)	0.61	381
R(20)	0.18	434
R(22)	0.11	381
R(24)	0.18	456

Table 1. Standard refractivity (right column) computed from index of refraction measurements in C_2H_4 at approximately 0.015 atmosphere pressure. Extinction parameter α obtained from cell transmission $\exp(-\alpha\ell)$ where ℓ is path length.

OZONE (3%) IN O_2, 9.6 μm CO_2 LASER BAND

line	α	$(n-1)\times10^6$
P(36)	0.201	295.1
P(34)	0.093	284.8
P(32)	0.174	275.9
P(30)	0.192	267.9
P(28)	0.276	284.6
P(26)	0.177	283.1
P(24)	0.021	278.6
P(22)	0.051	282.0
P(20)	0.168	275.3
P(18)	0.192	276.0
P(16)	0.270	277.8

Table 2. Standard refractivity (right column) computed from index of refraction measurements in O_3(3%) in O_2 at approximately 0.02 atmospheres. Extinction parameter α obtained from cell transmission, $\exp(-\alpha\ell)$, where ℓ is path length.

Figure 10 shows the final optical layout for this work, including the wavelength-monitoring spectrograph (C), the receiving sensors which are largely self-explanatory, and the two-chambered "bi-prism" (F) into which standard gases (such as N_2) and other gases such as ethylene could be put at differing pressures. The bi-prism has NaCl windows. Figure 11 is a photograph of the bi-prism showing the windows, separate chambers, and gas inlet-outlet-tubes. Pressure in the chambers was measured with a Barocell manometer, and temperature constancy was monitored with thermocouples.

The basic equation for the schlieren effect shows the relationship between focal spot deflection at the knife edge and the change of total optical path length along the beam. Since optical path length is the product of physical path and refractive index, it is possible to extract index values from a geometrically simple layout such as that shown in Figure 10. The concept of a gas bi-prism was borrowed from a well-known solid state technique. In our case, one cell is always filled with air and the other cell is evacuated and the location of the focal spots determined. This establishes two points on a smooth curve of second order, and automatically permits scaling of indices from beam spot displacement. When test gases are introduced into the bi-prism, their refractive indices are obtained in relation to this scale.

Figure 12 shows direct IR photographs of the bi-prism/schlieren image plane in two different situations. The triptych is particularly interesting because it demonstrates clearly the differing refractive properties of the two gases C_2H_4, 0.5 atmos. (upper chamber) and air (lower chamber). The top image is for a knife edge setting which passes the beams from both chambers of the bi-prism; the upper beam is blocked at an intermediate setting (middle image), and both beams are blocked for the setting pertaining to the lower picture. The other pair of pictures applies to a setup in which the upper chamber was evacuated and the knife edge oriented in the opposite direction, thus reversing the order of blocking the beam spots as the knife edge is traversed.

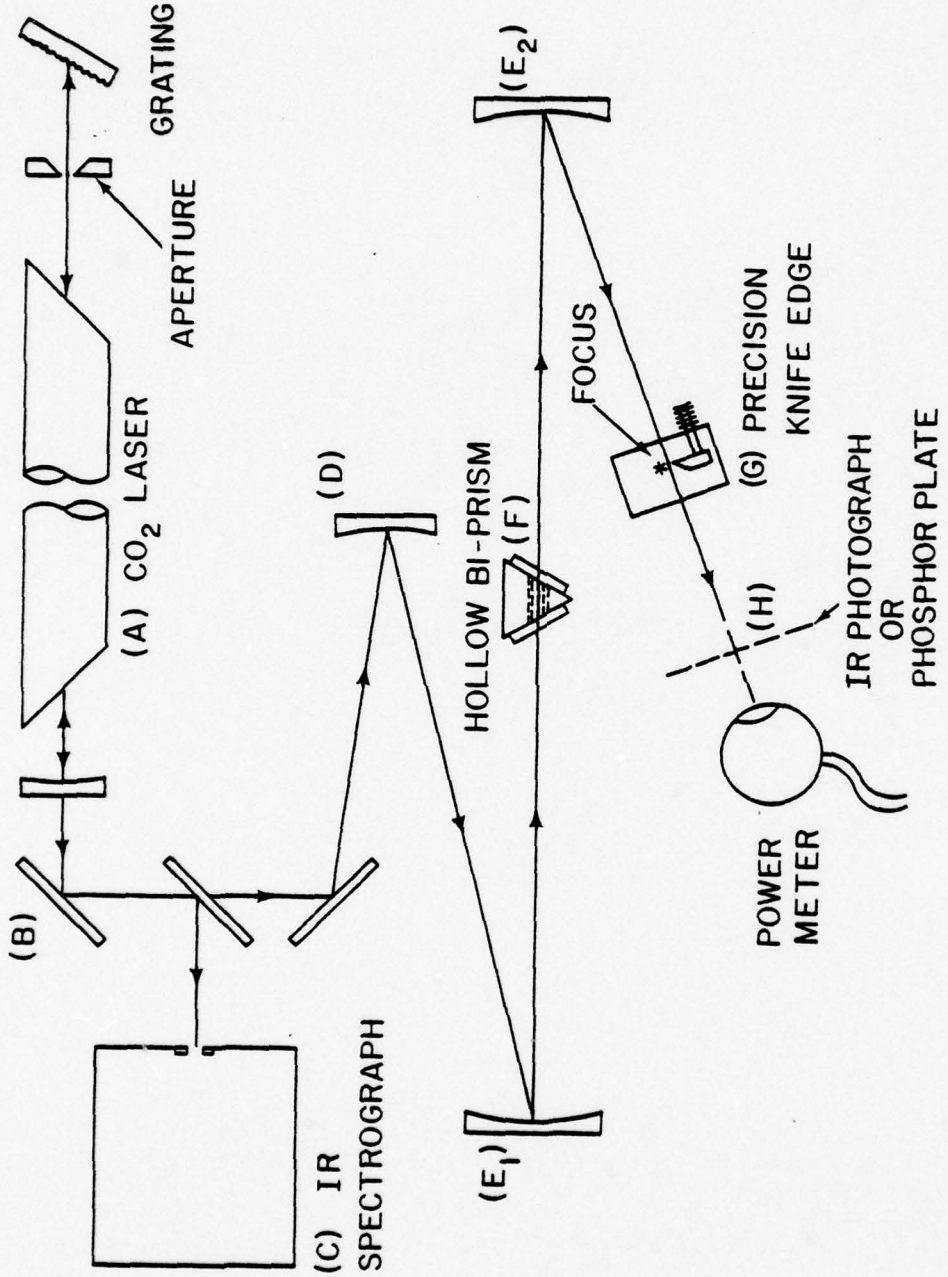


FIGURE 10

Final Optical Layout for IR Schlieren

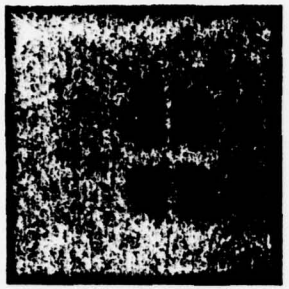
Versar inc.



FIGURE 11

Photograph of Hollow Bi-Prism Used in
Final Optical System

C_2H_4 in Upper Chamber
Air in Lower Chamber



Beams through both chambers



Upper beam blocked

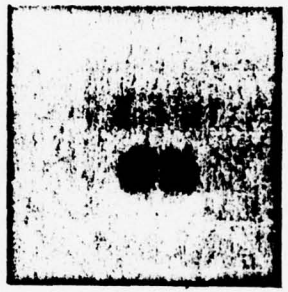


Both beams blocked

Upper Chamber Evacuated
Air in Lower Chamber



Beams through both chambers



Both beams blocked

FIGURE 12

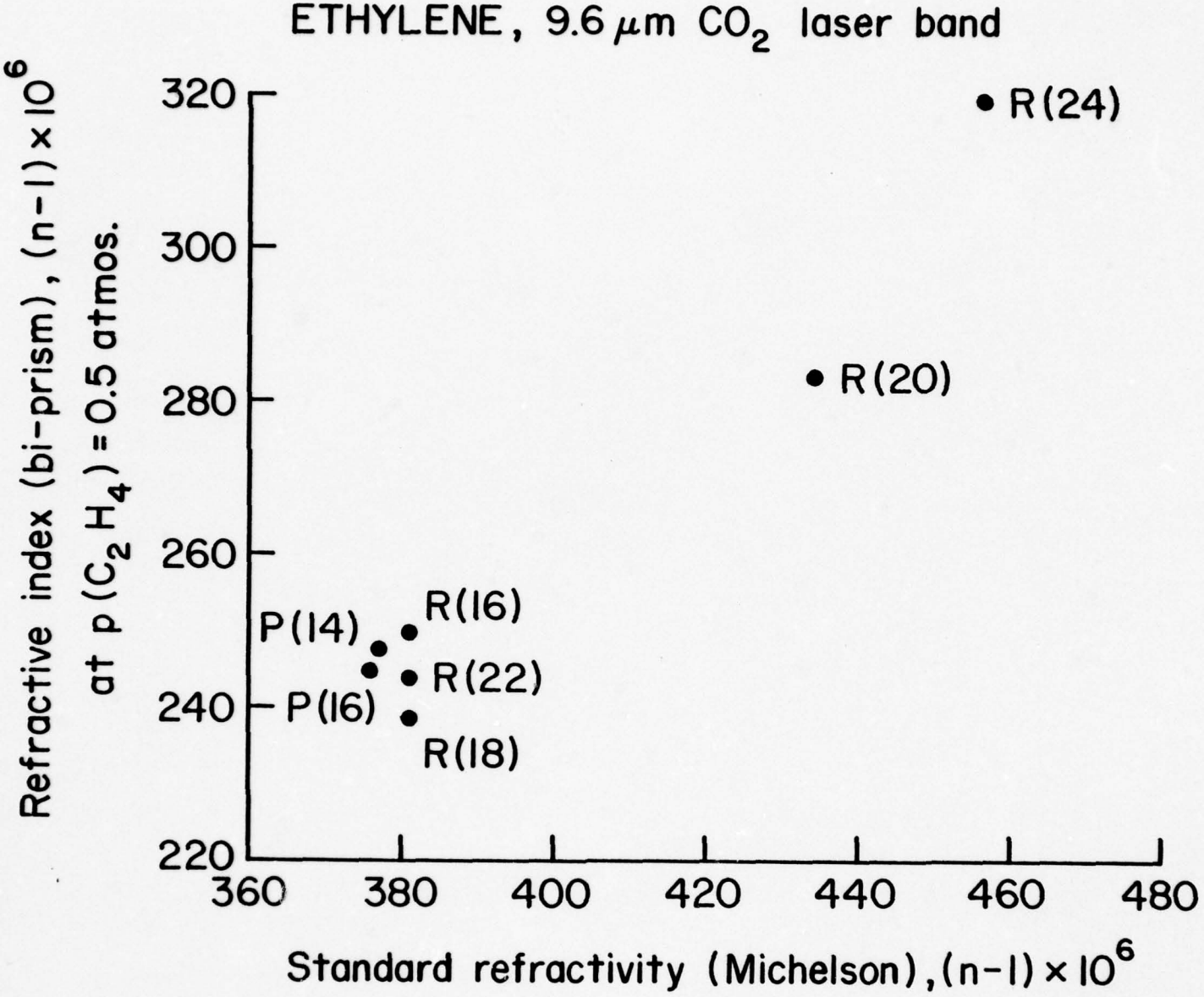
IR Photographs of the Bi-Prism/Schlieren Image Plane

The quantitative measurement of the beam spot deflection was made by means of half-intensity observations of the laser power passed by the knife edge; i.e., beam spot position was defined as that setting at which the power meter (Figure 10) read 1/2 of the full power for the laser line (and prism chamber) in question. Automatically included in these observations was a compensation for absorption in the gas in the bi-prism. Beam spot deflections were reduced to absolute refractive index by means of the calibrations described above.

The principal gas we studied was ethylene, both in the pure form and mixed with N_2. Figure 13 shows the very interesting comparison between data taken with the bi-prism method and data previously obtained with the Michelson interferometer. One immediately sees the correlation between the two, indicating that the bi-prism/schlieren technique sees much of the full variation of refractivity that one realizes is present in the same material under conditions of low pressure and high wavelength resolution. Passing through the CO_2 laser lines in order, the index excursions are very similar. Of course, the bi-prism measurements are not as informative in the sense of the basic physics of anomalous dispersion, but they have the advantage of being extremely simple to carry out — and they are, in fact, schlieren measurements that demonstrate the differential visibility of regions of varying optical pathlength, based on anomalous dispersion in molecular gases and which are recordable by a variety of IR imaging techniques.

FIGURE 13

Correlation between Refractive Index Measurements with Bi-Prism System and with Michelson Interferometer Techniques



REFERENCES

1. S.S. Penner, Quantitative Molecular Spectroscopy and Gas Emissions, Addison Wesley (1959).
2. A. Hadni, Essentials of Modern Physics Applied to the Study of the Infrared, Pergamon Press (1967).
3. M.V. Leykin and B.I. Molochnikov, Optical Technology 40, 782 (1973).
4. J.E. Sears and H. Barrell, Philos. Trans. A231, 75 (1932).
5. H. Barrell and J.E. Sears, Philos. Trans. A238, 1 (1939).
6. E.R. Peck and B.N. Khanna, J. O.S.A. 52, 416 (1962).
7. E.R. Peck and D.J. Fisher, J.O.S.A. 54, 1362 (1964).
8. E.R. Peck and B.N. Khanna, J.O.S.A. 56, 1059 (1966).
9. C.R. Mansfield and E.R. Peck, J.O.S.A. 59, 199 (1969).
10. E.R. Peck and K. Reeder, J.O.S.A. 62, 958 (1972).
11. R. Penndorf, J.O.S.A. 47, 146 (1957).
12. D.E. Snider and A. Goldman, "Refractive Effects in Remote Sensing of the Atmosphere with Infrared Transmission Spectroscopy", BRL Report No. R1790 (June, 1975).
13. H.J. Siebeneck, D.W. Koopman and J.A. Cobble, Rev. Sci. Instr. 48, 997 (1977).
14. D.W. Koopman, H.J. Siebeneck, G. Jellison, and W.G. Niessen, Rev. Sci. Instr. 49, 524 (1978).
15. K. Asai and T. Igarashi, Japan J. Appl. Phys. 14, Suppl. 14-1 (1975).
16. B.D. Green and J.I. Steinfeld, Environ. Sci. Technology 10, 1134 (1976).
17. E.D. Hinkley, Environ. Sci. Technology 11, 564 (1977).
18. A. Mayer, J. Comera, H. Charpentier, and C. Jaussand, Appl. Optics 17, 391 (1978).

APPENDIX A

Reprinted from APPLIED OPTICS, Vol. 15, page 1350, June 1976
Copyright 1976 by the Optical Society of America and reprinted by permission of the copyright owner

Infrared photography at 5 μm and 10 μm

Gene F. Frazier, T. D. Wilkerson, and J. M. Lindsay

When this work was done all authors were with Versar, Inc., Springfield, Virginia 22151; T. D. Wilkerson is with University of Maryland, Institute for Fluid Dynamics and Applied Mathematics, College Park, Maryland 20742. J. M. Lindsay is with Chesapeake Biological Laboratory, Solomons, Maryland 20668.
Received 9 March 1976.

Sponsored by Franklin S. Harris, Jr., Old Dominion University.

With the increased use of imagery, particularly with laser sources, it is desirable to have rapid and direct methods of ir photography. Such a technique is reported here, based on relatively unexplored properties of silver halide emulsions. This new effect involves the sensitization and desensitization of silver halide films by ir radiation. The process is fundamentally different from such ir photographic reversal effects as the Herschel effect. Our experiments have used low power, cw, CO and CO_2 lasers providing film irradiance in the range of 0.1–1W/cm^2, at wavelengths near 5 μm and 10 μm. The technique offers greater sensitivity and dynamic range than foot-print paper[1] and does not require taking a picture of a picture as with liquid crystals or with ir image plates,[2] which operate by desensitized fluorescence.

Different photographic regimes have been established and are illustrated in Fig. 1. The principal one [Fig. 1(a)] consists of an ir exposure (t_0–t_1) which is immediately followed by a visible exposure V of the entire film. Upon development, the film is found to have been *desensitized* to visible light in the regions of ir exposure. For each level of power density leading to desensitization, there is a shorter ir interval (t_0–t_2) giving *sensitization* to visible light, which may be related to classical

thermal sensitization. If sufficient time elapses (a few seconds) between the ir and visible exposures [t_0–t_3 in Fig.1(c)], both the sensitizing and desensitizing effects disappear. It appears that prior ir illumination modifies the processes that can take place in a conventional film, so the film's response to visible light is temporarily but appreciably altered. The present sensitivity of this effect to ir light is satisfactory for many purposes of laser research. Infrared sensitivity may be increased by manipulating the many film factors that have usually been chosen to optimize the visible response. The ir intensity and exposure time are to some extent interchangeable in the classical sense of reciprocity; thus an ir photograph of this type will yield isointensity contours for describing laser modes and far-field transmission patterns.

Since there are two exposures involved, each having its own wavelength and duration, the full specification of characteristic (H and D) curves can be very complex. Here we give data on an extremely useful photographic material, Polaroid 55 PN (positive/negative) film and demonstrate the effects of varying (1) the ir exposure time at fixed intensity, and (2) the wavelength of the visible postexposure.

Figure 2 summarizes the net photographic densities obtained on Polaroid 55 PN *negatives* over a range of ir exposure times at a measured power density at the film of 0.3W/cm^2. The two curves represent the use of (a) filtered green light or (b) white light as the visible postexposure. Little visible light is required to establish the best background density; i.e., that giving the greatest contrast to the ir effect. The white light exposure (b) was made with an apertured, battery-powered incandescent lamp several meters from the film; this exposure was $\frac{1}{50}$ second at an average power density of 1 μW/cm^2 measured at the film plane. The green light exposure (a) used the same lamp filtered for the region $\Delta\lambda$ = 0.56–0.57 μm, and with the film exposure adjusted to give the same background density as in the white light case.

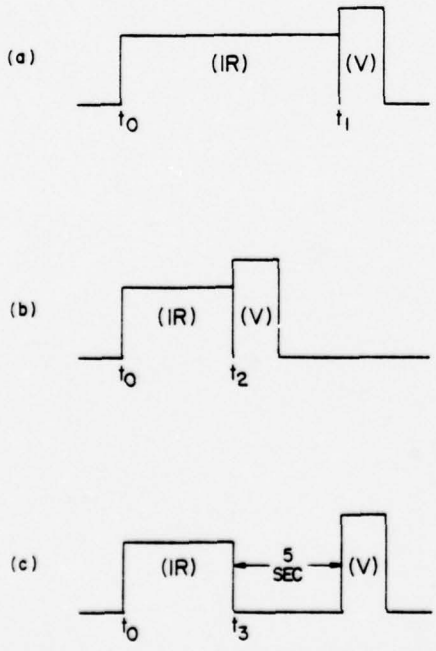


Fig. 1. Exposure sequences employed in ir photography via modification of sensitivity to visible light: (a) desensitization, (b) sensitization, (c) no influence by ir. Intensity scales are arbitrary.

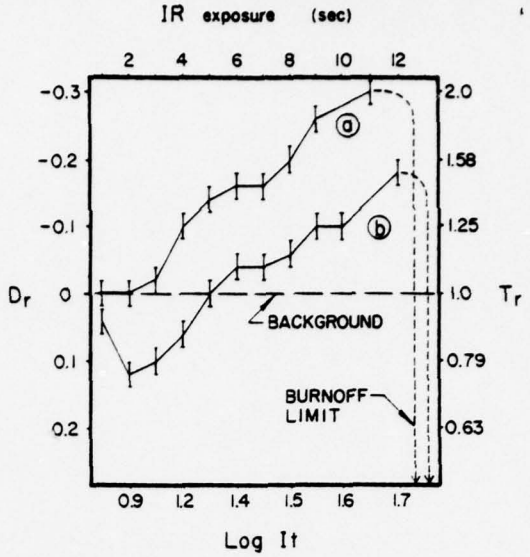


Fig. 2. Characteristic curves for ir modification of visible sensitivity, for (a) green light, (b) white light at ir power density = 0.3 W/cm^2.

Image density relative to the background density is shown in Fig. 2, vs the ir exposure time, with blackness of the negative increasing downward. The principal effect is desensitization ($D_r < 0$); i.e., the *print* is blacker than the background wherever the ir exposure has been sufficiently great.

The white light curve (b) displays all the regions described above; the *sensitization* regime covers the ir exposure interval 1–5 sec, and *densensitization* 5–12 sec. Photographic effects of the ir light are visible using ~$\frac{1}{10}$ the exposure required to burn the film. By filtering to obtain a green postexposure, the sensitization regime is suppressed and a considerable range of desensitization contrast is obtained for exposures several times less than the burn threshold. We have also discovered an effect leading solely to sensitization. It appears that we are dealing with two processes within the emulsion that set in at different rates and have opposing effects on silver precipitation.

The process works for many silver halide films, as will be detailed in a subsequent paper; and its dependence on the wavelength of the visible exposure provides a useful control over the net photographic densities obtained.

All the conventional films we have tried demonstrate similar regimes of ir influence on latent image formation. The highest sensitivity (0.1 W/cm^2) to ir light was obtained with Polacolor 108 and Kodacolor II. This is equivalent to photographing the 1-mm^2 beam spot of a 1-mW laser. Infrared sensitivity may be improved by making films with less of the chemical stabilizers that optimize the films for everyday photography.

Among the advantages of this technique is that it provides a convenient, permanent record of the intensity distribution of laser output. In addition to intensity measurements, we have used the method to record dispersed line spectra of CO and CO_2 lasers. Since the technique is used directly on the optic axis, no distortion is introduced by copying optics (as in most liquid crystal and fluorescent display systems). This allows for greater accuracy in relative position or wavelength measurements. At present, linear resolution is better than 6–8 line pairs/mm for most conditions.

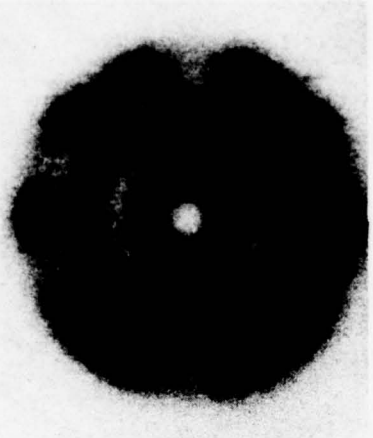


Fig. 3. Photograph of a CO_2 laser mode pattern. Power density in the dark regions is 0.35–0.45 W/cm^2. Exposure time is 3 sec on Polaroid 55 PN film.

This technique might be attractive for rapid photography of far-field, high energy laser mode patterns. Note that the exposure times employed are comparable with the running time of a gas-dynamic ir laser and that a nominal midrange of useful sensitivity (~0.4 W/cm^2) is equivalent to a 1-kW laser beam 50 cm in diameter.

A CO_2 laser mode photograph appears in Fig. 3. This Polaroid 55 PN print shows an unstable pattern that was degenerated from TEM_{20} by adjusting the cavity mirrors. Intensity in the dark regions is 0.35–0.45 W/cm^2; the print is an enlargement over the actual beam diameter (~15 mm).

So far, the optimum ir parameters have been determined largely by trial and error. To obtain major gains in sensitivity, the main mechanisms need to be identified and manipulated accordingly. Two main lines of enquiry seem to be the most promising: (1) better delineating the interaction between ir radiation and the gelatin (i.e., nonsilver halide materials) contained in the emulsion, and (2) estimating the net influence of ir irradiation on the drift mobility and lifetimes of photogenerated species within the grains. At the macroscopic level both (1) and (2) may be expressed in terms of latent image formation and fading. If, for example, important grain–gelatin-dye interactions can be disrupted by ir radiation, the surface latent image will surely be affected—and most probably in the direction of desensitization. This idea finds support in the evidence that those films for which surface image formation predominates are also those that are most effective for middle ir recording. Prospects for sensitization, on the other hand, may be found in the effect of a temperature change on the water-gelatin complexes involved in latent image formation and the effect of temperature on silver halide absorption bands.

Although the photoelectric absorption by silver halides lies in the visible, the well depth of important internal traps for photoelectrons is commonly of order 0.04 eV within the grain.[3,4] This is comparable with the temperature energy in a heated crystal, so the internally trapped electrons are susceptible to thermal reejection. This will influence the drift mobility, rates of recombination, and the lifetimes for electrons and holes. That these quantities are *different* functions of temperature[3,5] for electrons vs holes implies the possibility of competing effects that would yield sensitization or desensitization depending on the ir irradiation level. Some heating must be present since residual ir effects can be recorded when the visible flash occurs 1–2 sec *after* the ir exposure. A temperature-related mechanism is being considered, but we feel that more is involved. The exact role of the thermalization may be assessed through experiments like those of Babcock *et al.*[6] (who studied the effect of moderate temperatures on sensitized emulsions), as extended to higher temperatures and heating rates.

The present problems involved in developing a usable photographic model are difficult since the ir exposure only *interferes* with, rather than initiates, the image forming process. Therefore the uncertainties in the normal photochemical steps are compounded by complex ir exposure effects. As we have suggested, a study of the interaction of ir radiation with the gelatin and/or grain interior may help to clarify the ir mechanism. Toward this goal we are attempting to correlate the better known properties of emulsions to produce a first order model of the new process to produce a new film with characteristics optimized for use in the middle ir. Our early results are presented here to stimulate further research and to report a new and useful ir recording method. More data on techniques and models will be given in a future paper.

The authors gratefully acknowledge the review of this paper by Franklin S. Harris, Jr., of Old Dominion University, and the suggestions as to content by him, Richard Adams, and Robert White (of NASA Langley Research Center). This research was supported by AFOSR under contract F44620-72-C-0076.

References

1. Korad Division of Hadron, Inc., Santa Monica, California.
2. Optical Eng., Inc., Santa Rosa, California.
3. J. Malinowski, Photogr. Sci. Eng. 14, 112 (1970).
4. F. C. Brown and K. Kobayashi, J. Phys. Chem. Solids 8, 300 (1959).
5. John S. Wei and Frederick C. Brown, Photogr. Sci. Eng. 17, 197 (1973).
6. T. A. Babcock, W. C. Lewis, P. A. McCue, and T. H. James, Photogr. Sci. Eng. 16, 104 (1972).

A NEW METHOD OF IR PHOTOGRAPHY

by

Gene F. Frazier

PROCEEDINGS OF SOC. PHOT. INSTR. ENG.

VERAR INC.

March 22-23, 1976
Reston, Virginia

Introduction

With the increased use of infrared imagery, particularly with laser sources, it is desirable to have rapid and direct methods of infrared photography. Such a technique is reported here, based upon relatively unexplored properties of silver halide emulsions. This new effect involves the sensitization and densensitization of silver halide films by IR radiation. The process is fundamentally different from such infrared photographic reversal effects as the Herschel effect. Our experiments have been conducted using low power, cw, CO and CO_2 lasers providing film irradiance in the range of 0.1-1W/cm^2, at wavelengths near 5 and 10μm.

We have adopted the new process for routine IR schlieren photography of gas flows. The technique offers greater sensitivity and dynamic range than "foot print paper"[1], and does not require taking a picture of a picture as with liquid crystals, or with IR image plates[2] which operate by desensitized fluorescence.

Different photographic regimes have been established; these are illustrated in Figure 1. The principal regime (Fig. 1a) consists of an IR exposure interval (t_o-t_1) which is immediately followed by a short visible exposure (V) of the entire film. Upon development, the film is found to have been <u>densensitized</u> to visible light in the regions of IR exposure. For each level of power density leading to desensitization, there is a shorter infrared exposure interval (t_o-t_2) which yields <u>sensitization</u> to

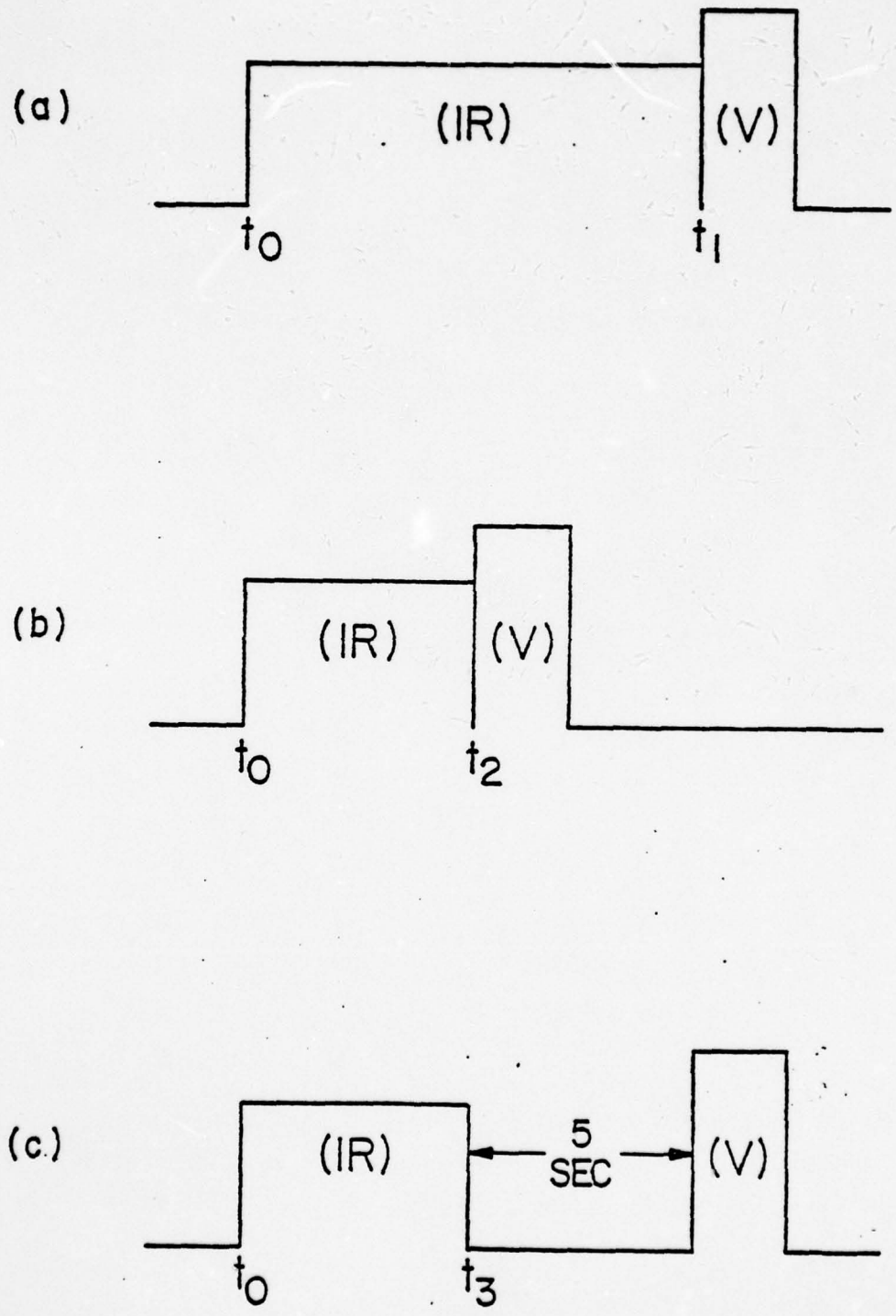


FIGURE 1. Exposure sequences employed in IR photography via modification of sensitivity to visible light: (a) desensitization, (b) sensitization, (c) no influence by IR.

visible light, which may be related to classical thermal sensitization. If sufficient time is allowed to elapse (a few seconds) between the IR and visible exposures (t_0-t_3 in Fig. 1b), both the sensitizing and desensitizing effects disappear.

It appears that infrared illumination modifies the processes that can take place in a conventional film, in such a way that the film's response to visible light is temporarily but appreciably altered. The present sensitivity of this effect to infrared light is satisfactory for many purposes of laser research. Sensitivity can likely be increased by manipulating the many film factors which heretofore have usually been chosen to optimize the response to visible light.

In Section 2 we will discuss characteristic curves relating final photographic density to infrared exposure time and to the wavelength of visible light employed. Data on Polaroid film are presented. Section 3 describes the appearance of IR photographs in which the IR image intensity varies; intensity and exposure time are to some extent interchangeable in the classical sense of reciprocity. Thus an IR photograph of this type can yield iso-intensity contours which are useful in describing laser modes and far-field transmission patterns. The process works for many silver halide films, as will be detailed in a subsequent paper, and its dependence on the wavelength of the visible exposure provides a useful control over the net photographic

densities obtained.

Characteristic Curves

Since there are two exposures involved in this process, each having its own wavelength and duration, the full specification of characteristic (H. & D.) curves can be very complex. This section gives illustrative data on an extremely useful photographic material, Polaroid 55 PN (positive/negative) film, and demonstrates the effects of varying (i) the IR exposure time at fixed intensity, and (ii) the wavelength of the visible post-exposure.

Figure 2 summarizes the net photographic densities obtained on Polaroid 55 PN negatives over a range of IR exposure times at a measured power density at the film of $0.3 W/cm^2$. The two curves represent the use of (a) filtered green light or (b) white light as the visible post-exposure. Very little visible light is required to establish the most favorable background density; i.e., that which imparts the greatest contrast to the IR effect. The white light exposure (b) was made with an apertured, battery-powered incandescent lamp several feet from the film; this exposure was 1/50 second at an average power density of $1 \mu W/cm^2$ measured at the film plane. The green light exposure (a) used the same lamp filtered for the region $\Delta\lambda = 0.56 - 0.57 \mu m$, and with the film exposure adjusted so as to give the same background density as in the white light case.

Image density relative to the background density is shown in

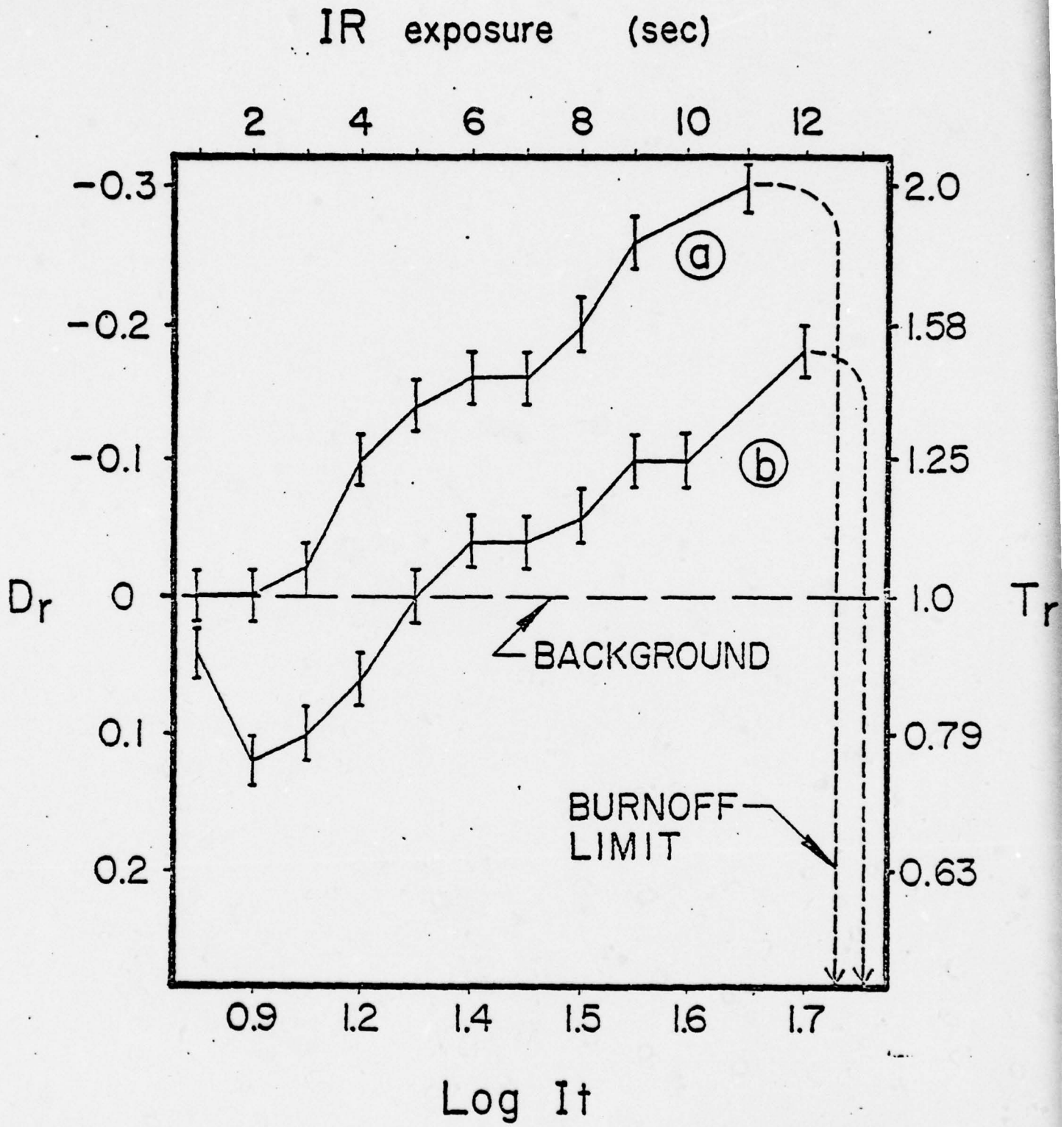


FIGURE 2. Characteristic curves for IR modification of visible sensitivity, for (a) green light, (b) white light at IR power density = 0.3 mW/cm^2.

Figure 2, vs. the IR exposure time, with blackness of the negative increasing downward. The principal effect is desensitization ($D_r < 0$), which renders the print blacker than the background wherever the IR exposure has been sufficiently great.

The white light curve (b) displays all the regions described in Section 1; the sensitization regime covers the IR exposure interval 1-5 seconds, and desensitization 5-12 seconds. Photographic effects of the infrared light are visible using ~ 1/10 the exposure required to "burn" the film. By filtering to obtain a green post-exposure, the sensitization regime is suppressed and a considerable range of desensitization contrast is obtained for exposures several times less than the burn threshold. We have not yet discovered an entirely opposite effect, namely some procedure which would lead exclusively to sensitization. It appears that we are dealing with two processes within the photographic emulsion which set in at different rates and have opposing effects on silver precipitation.

All the conventional and Polaroid films we have tried demonstrate these regimes of IR influence on latent image formation with similar degrees of effectiveness. The highest sensitivity ($0.1\ W/cm^2$) to infrared light has been obtained with Polacolor 108 and Kodacolor II. This is equivalent to photographing the $1\ mm^2$ beam spot of a 1 mW laser. We believe that IR sensitivity will be improved by making films that contain fewer chemical stabilizers, which have traditionally been added to optimize the

films for everyday use with visible light.

Photography and Photometry

A type of reciprocity law holds for the infrared sensitivity; i.e., for exposure times at least in the range 1-10 seconds, it is the product (image intensity) x (exposure time) that determines the density D_r relative to background. Therefore the curves in Figure 2 may also be thought of as representing the variation in film blackening in an IR snapshot of an image whose intensity varies with position.

In addition to the ordinary type of photographic photometry that could be carried out on the basis of curve (a) in Figure 2, one can take advantage of the two regimes in curve (b) for qualitative photometric interpretation of IR photographs. For example, we have photographed dispersed line spectra of the CO_2 laser which show white and black spectral lines owing to the IR intensities falling on one side or the other of the crossover from sensitization to desensitization. This type of photography provides a convenient record of the intensity distribution of the laser output.

Another application is isophotometry of a complex IR image. A contour of constant, intermediate intensity can be identified by looking for curves bounded by black and white areas and having the same density as the background. Several isophotes can be so photographed, by varying the IR exposure time. This places

different intensities at the crossover condition, and sufficies to label these isophotes with intensity values, to the extent that reciprocity holds.

This technique may be very attractive for rapid photography of far-field, high energy laser patterns. Note that the exposure times employed are comparable to the running time of a gas-dynamic infrared laser.

Figure 3 illustrates the appearance of a single mode laser beam spot when photographed by this method. Scans with a calibrated pyroelectric detector verified the bell-shaped profile (3a), while the photographic crossover gives one the impression of a doughnut-shaped mode structure (3b, 3c). The quantity D in Figure 3c is the density of the Polaroid 55 PN negative whose print is shown in Figure 3b. Regime R_1 represents sensitization to the low IR intensity in the "wings" of the laser profile. Closer to the beam center, this reverses into densensitization (R_2), and the locus of points on the (R_1, R_2) boundary constitutes an isophote of the type discussed above. A higher intensity isophote could be visualized using the crossover from R_2 to R_3 (burnoff).

From this illustration of the principle, it is clear that the "crossover isophotes" and the attendant white and black patches can be very useful in interpreting a complicated laser beam pattern, without the expense of a multi-element array of detectors.

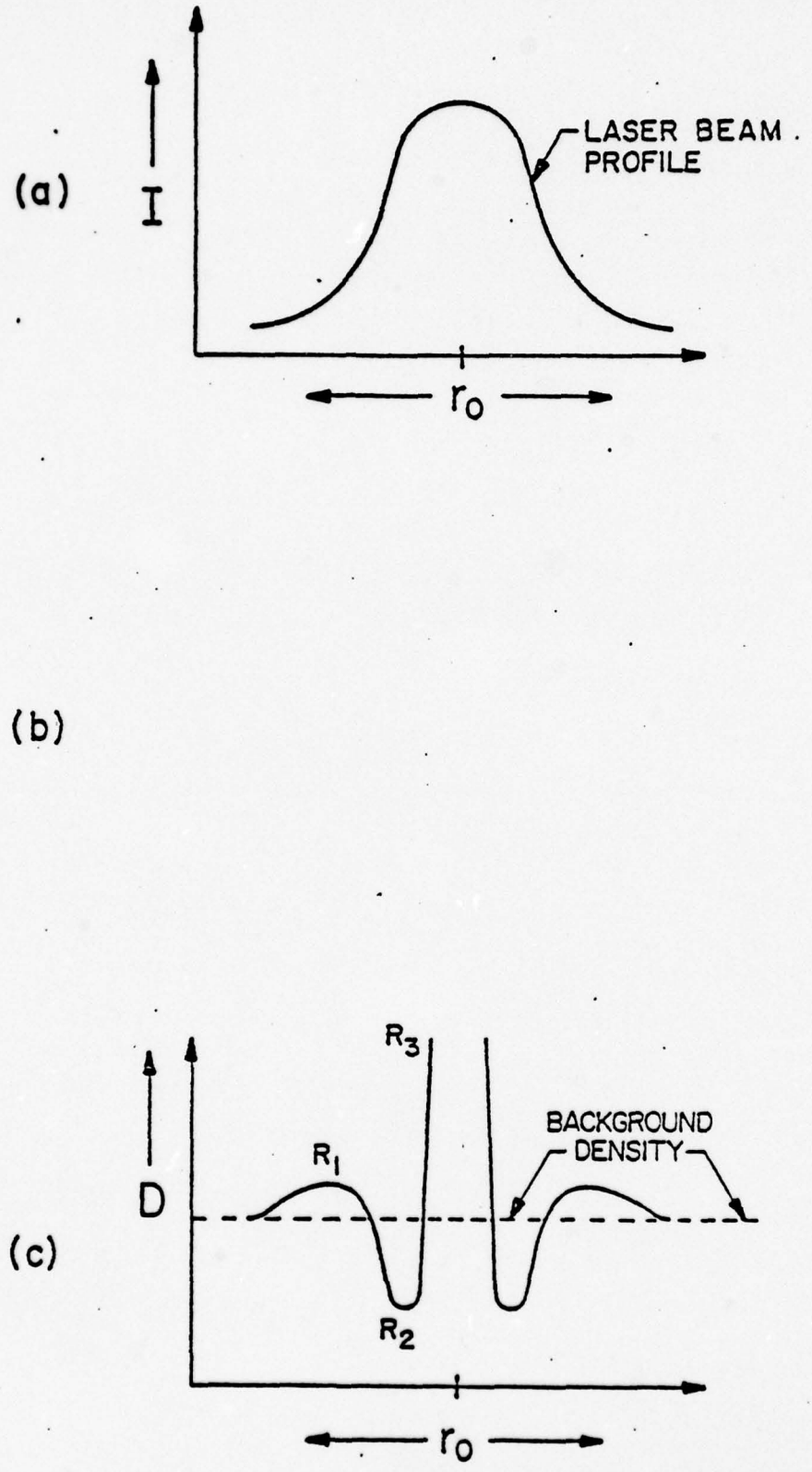


FIGURE 3. Sensitization vs Desensitization effects of infrared produced annular image of Gaussian beam spot: (a) Gaussian beam profile, (b) the print of the negative, (c) showing three IR intensity regimes.

The present sensitivity and dynamic range are suitable for study of 1 kW infrared laser outputs with a beam spot diameter of order one foot.

Discussion of Possible Mechanisms

We have found that, in order to obtain good quality infrared photographs, exposures longer than 10 seconds are required for incident IR power densities of 0.15 W/cm^2 or less. This would be an even more useful process if one could improve the IR sensitivity by a few orders of magnitude.

So far the optimum photographic parameters have been discovered largely by trial and error. To obtain major gains in sensitivity requires that the principal mechanisms be identified and manipulated accordingly. By a process of elimination, two main lines of future enquiry have emerged.

We believe the most promising directions are: (A) better delineating the interaction between IR radiation and the gelatin (i.e. non-silver halide materials) contained in the emulsion, and (B) estimating the net influence of IR irradiation on the drift mobility and lifetimes of photochemical species within the grains.

(A) Gelatin (grain boundary)

It is generally believed that gelatin plays some role in the photographic process, while the degree and exact nature of its importance are unclear. A principal function of gelatin may be to localize and promote the action of sensitizers, which can greatly influence the probability of latent image formation on the surface

of the photographic grains. Gelatin components themselves may also facilitate the escape of photogenerated bromine from a grain, and thereby reduce chemical attack on the surface latent image. If important grain-gelatin-dye interactions can be disrupted by infrared radiation, the surface latent image will surely be affected -- and most probably in the direction of desensitization. This idea finds support in the evidence in that those films for which surface image formation predominates are also those are most effective for middle infrared recording. Prospects for sensitization, on the other hand, may be found in the effect of a temperature change on the water-gelatin complexes involved in latent image formation.

(B) Grain Interior

Here attention is drawn to whether infrared radiation is directly absorbed in a grain, or is there indirect heating via the gelatin environment -- and, if so, what effects result at the latent image level.

So far we have been unable to obtain infrared absorption data for the silver halide grain material employed in the manufacture of commercial films. Since real grains likely contain trace impurities,[3,4] for the purposes of photographic effects not attainable with pure silver halides, grain absorption cannot be inferred solely from data on the pure substances. The films we have studied exhibit broad absorption features throughout the

infrared, some of which lie in the CO and CO_2 laser emission bands. However, even if direct IR absorption by grains is unlikely, one can surmise lattice excitations in the grain due to thermal conduction from the surrounding gelatin.

Although the photoelectric absorption by silver halides lies in the visible, the well depth of important internal traps for photoelectrons is commonly of order 0.04 eV within the grain[4,5]. This is comparable to the temperature energy in a heated crystal, so that the internally-trapped electrons are very susceptible to thermal re-ejection. This will influence the drift mobility, rates of recombination, and the lifetimes for electrons and holes. That these quantities are <u>different</u> functions of temperature[4,6] for electrons <u>vs</u>. holes holds open the possibility of counter-vailing effects which would yield sensitization or desensitization depending on the infrared irradiation level. Some heating must be present since residual infrared effects can be recorded when the visible flash occurs 1-2 seconds <u>after</u> the infrared exposure. A temperature-related mechanism is being considered but it is clear that more is involved. Babcock[7], <u>et al</u>., for example have made extensive measurements of the temperature dependence of the photographic process. These results would not suggest desensitization (R_2) but rather sensitization at higher infrared exposure, i.e., higher temperature.

(C) Conclusion

The present problems involved in developing a usable photographic model arise from the fact that the infrared exposure only interferes with, rather than initiates the image forming process. Therefore the uncertainties in the "normal" photochemical steps are compounded by complex infrared exposure effects. As we have suggested, a study of the interaction of infrared radiation with the gelatin and (or) grain interior may help to clarify the infrared mechanism. Toward this goal we are attempting to correlate the better known properties of emulsions to produce a first order model of the new process, in order to produce a new film with characteristics optimized for use in the middle infrared. Our early results are presented here to stimulate further research. More data concerning techniques and models will be presented in a future paper.

References

1. Korad Division of Hadron, Inc., Santa Monica, Ca.
2. Optical Eng. Inc., Santa Rosa, Ca.
3. V. Platikanova and J. Malinowski, Phys. Status Solidi, 14, 205 (1966).
4. J. Malinowski, Photogr. Sci. Eng., 14, 112 (1970).
5. F. C. Brown and K. Kobayashi, J. Phys. Chem. Solids, 8, 300 (1959).
6. John S. Wei and Frederick C. Brown, Photogr. Sci. Eng., 17, 197 (1973).
7. T. A. Babcock, W. C. Lewis, P. A. McCue, and T. H. James, Photogr. Sci. Eng., 16, 104 (1972).

Journal of Applied Photographic Engineering
Volume 3, Number 1, Winter 1977

Middle Infrared Photography Using Silver Halide Films

Gene F. Frazier

Abstract A method is described for silver halide photography at infrared wavelengths of approximately 5 and 10 μm, using laser sources. The technique involves sensitization and densitization of films to visible light as a result of pre-exposure to infrared radiation. Three different photographic regimes are established, depending on infrared intensity and length of exposure. Lines of study are suggested for further improvement of infrared sensitivity and dynamic range.

Journal of Applied Photographic Engineering 3: 31–34 (1977)

Introduction

As the use of infrared lasers becomes more and more widespread the need for methods for recording infrared images becomes more acute. Many attempts have been made in the past to extend the normal sensitivity range of silver halide films to accommodate these requirements. The use of photosensitive dyes has been of considerable benefit in the regions out to about 1.2 μm. Unfortunately the region beyond 2 μm has remained inaccessible, partly due to thermal interference with dye action.

Reported here is a technique which to some extent sidesteps the considerations of photochemical sensitivity *per se* and makes use of the effects of the physical environment on photographic response. Selective modification of ambient conditions at the grain usefully alters the normal photographic processes. This new method involves the sensitization and desensitization of silver halide films by infrared radiation in the 5 and 10 μm region. The technique offers greater range than footprint paper[1] and is less complex than liquid crystals or thermal plates in that no additional photograph is required to produce a permanent record.[2]

Experiments

The experiments were performed using low power, CW, CO, and CO_2 lasers providing focal plane irradiance of 0.1–100 W/cm^2, at wavelengths near 5 and 10 μm.

Different photographic regimes have been established and are illustrated in Fig. 1. The principal regime (Fig. 1*a*) consists of an IR exposure ($t_0 - t_1$) of the entire film, which is immediately followed by a visible flash. Upon development, the film is found to have been *desensitized* to visible light in the regions of IR exposure. For each level of power density leading to desensitization, there is a shorter infrared interval ($t_0 - t_2$) giving *sensitization* to visible light, which may be related to classical thermal sensitization. If sufficient time elapses (a few seconds) between the IR and visible exposures ($t_0 - t_3$ in Fig. 1*c*), both the sensitizing and desensitizing effects disappear. In general, the net effect of infrared exposure decreases as the delay between IR and visible exposure increases. It appears that prior infrared illumination modifies the processes that can take place in a conventional film, so that the film's response to visible light is temporarily but appreciably altered. The present sensitivity of this effect to infrared light is satisfactory for many purposes of laser research. IR sensitivity may be increased by manipulating the many film factors which have usually been chosen to optimize the visible response.

Figure 2 illustrates the experimental arrangement for the photographic testing. Flat mirrors (b) and (c) directed the laser output to the concave mirror (d), which then focused the beam to the plateholder (e). Laser power was measured with a calibrated PY-3 Harshaw detector (f). Total laser power was measured at 10-min intervals as a check for laser stability, which was found to be better than 5%. Infrared intensity was altered by changing the gas proportions in the discharge tube and by adjusting the power supply output current.

Image plates[2] and liquid crystal sheets were used to display the infrared images prior to insertion of the filmholder into the focal plane.

A tungsten light source (g) was located 2 m distant from the plateholder. Its integrated spectra irradiance was variable from 0.01 to 10 erg/cm^2/sec at this distance over the band of 0.4–0.7 μm.

Mechanical shutters were used to insure reproducibility of infrared and visible exposure times, although usable photographs were taken employing less precise methods of control.

In general, the photographic procedure begins with unexposed film and consists of two steps: (1) An initial exposure of the film to an infrared image, and (2) An additional exposure to visible light.

The exact length and temporal position chosen for the infrared and visible exposure times depends upon a number of parameters, notably infrared irradiance and film type. Various films were used to bring out different features of the effect. Polaroid films were studied in detail due to their convenience while other films were used to ascertain that operationally the same effects could be observed with these as with the Polaroid process films.

For the generation of contrast curves, the laser beam was used both as source and target image, due to its clean Gaussian profile and convenient size. The sensible diameter varied

The author is with Versar, Inc., 6621 Electronic Drive, Springfield, VA 22151.

Research supported by AFOSR Contract No. F44620-72-C-0076.
Original manuscript received April 15, 1976.
Accepted for publication June 22, 1976.

© 1977, Society of Photographic Scientists and Engineers.

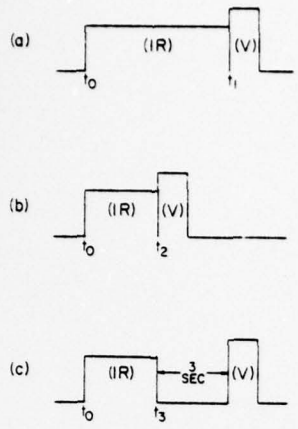


Figure 1. Exposure sequences employed in IR photography *via* modification of sensitivity to visible light: (*a*) desensitization, (*b*) sensitization, (*c*) no influence by IR. Intensity scales are arbitrary.

between 10 and 25 mm, depending upon the desired central power density and mode structure.

Prior to each exposure, power at the center of the infrared beam was measured using the pyroelectric detector. In addition all density measurements were made with a limiting aperture matching the active area of the pyroelectric detector (2 mm^2). This procedure simplified the task of relating optical density on the negative to power density at the focal plane. In general two density values were obtained for each negative; (1) optical density at the center of the IR image, and (2) contrast between the infrared image center and the background produced by the visible exposure. Contrast is defined here as the difference in density (ΔD) between the IR image and background.

It was learned early in the experiments that contrast decreased markedly if the density of the background rose above (0.7–0.8). It was found by experiment that optimum contrast was usually achieved for negatives sufficiently exposed to produce a background density of (0.5–0.6). For our experiments with Polaroid 55 PN this density was reached for white light exposures of 0.1 sec, using the source described above.

Figure 3 illustrates the three regimes of IR image recording encountered in this study. The film used here and for the contrast curve (Fig. 4) was Polaroid 55 PN, which provides a positive print and working negative.

Figure 3*b* shows a print made from a negative which had been exposed to the laser beam spot at a central irradiance (E_{IR}) of 0.3 W/cm^2 for 6 sec. Exactly at the end of the infrared exposure a $\frac{1}{10}$-sec flash of white light was added using the source described above, causing the overall exposure of the background, as shown.

The profile of the laser beam which produced this photograph is shown schematically in (Fig. 3*a*). In practice the radial distance at which the profile drops to zero intensity roughly

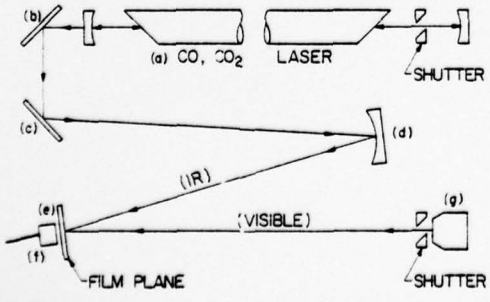


Figure 2. Experimental arrangement for infrared photography *via* modified sensitivity to visible light.

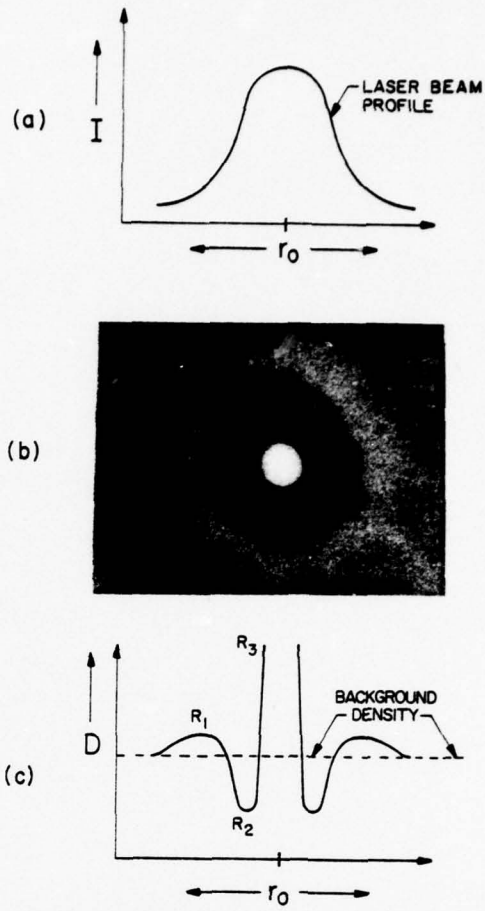


Figure 3. Sensitization vs Desensitization effects of infrared produced annular image of Gaussian beam spot: (*a*) Gaussian beam profile, (*b*) the print of the negative, (*c*) showing three IR intensity regimes.

corresponds to the observed radius of the infrared image on the negative.

Figure 3*c* shows the important relation between optical density and infrared intensity for the negative which produced the print in Fig. 3*b*. The density is plotted as a function of radius from the center of the negative image. The shape of this curve at $r \neq 0$ corresponds to effects observed on either side of the IR profile maximum. Passing from the periphery to the center of the image in Fig. 3*b*, the three evident regimes are:

1) Sensitization (outer white annulus)

$$E_{IR} \simeq 2 \text{ mW/mm}^2$$

2) Desensitization (dark ring)

$$E_{IR} \simeq 3 \text{ mW/mm}^2$$

3) Emulsion breakdown (central spot)

$$E_{IR} \simeq 4 \text{ mW/mm}^2$$

As each of these intensity regimes occur, a change is observed in the density profile (Fig. 3*c*). The sensitization regime corresponds to a density on the negative which is slightly *higher* than the surrounding background. The desensitization regime is observed at higher intensity and produces a developed negative which is more *transparent* than the background. Regime 3 occurs at IR energies which destroy part of the emulsion and cause the bleaching of the Polaroid negative.

It was also discovered that silver halide films such as Kodak Panatomic-X and Plus-X displayed effects similar to those

of the Polaroid films but slightly inferior in terms of contrast. There is also data which suggests that infrared effects may increase with decreasing emulsion thickness. Regime 3 closely resembles the "burnoff" of Polaroid films by dye laser action but the exact understanding of this effect is not clear. The three regimes were tested for reversibility, i.e., the film was exposed to infrared images and a short time was allowed to elapse between the end of the infrared and beginning of the visible exposures. It was observed that regime 3 is "irreversible," i.e., the same result is observed for very long delays (1 hr). The exact nature of this regime is unclear and will require further study. Regimes 1 and 2 are reversible, i.e., if more than 6 sec are allowed to elapse between IR and visible exposures, virtually all infrared effects disappear. Indeed, prior to the addition of shutters for controlling exposure times, much of the early data lacked reproducibility, which was later directly related to the effects of relaxation on photographs with precisely controlled variable delay times. In addition, it was observed that IR exposure of the emulsion after the visible exposure produces no discernable effects. Data involving the relaxation times for the sensitization and desensitization effects will be presented in a future paper.

Except in the exposure region of regime 3, the infrared produces no discernable image of its own, but rather determines the effectiveness of a following visible exposure. For this reason we must discuss film effects based upon measurements of relative density (i.e., contrast) between the IR image and the background.

Figure 4 shows relative density curves, adjusted to constant background, for Polaroid 55 PN negatives. In Fig. 4, (D_r) corresponds to the relative density ($D_I - D_B$) between the density of the background (D_B), measured in the region surrounding the infrared image, and the density of the IR image measured in the region of infrared radiation. Infrared induced desensitization is indicated by a higher print density and negative relative densities in Fig. 4. Figure 4 has been normalized to zero background density to show relative density, the true background density is 0.5 for all exposures. The true IR image density may be found by adding 0.5 to a specific D_r value in Fig. 4. Both relative transparency (T_B/T_I) and relative density ($D_I - D_B$) are plotted as a function of infrared exposure time. For each of the photographs used to produce curve (*b*) the visible exposure was maintained at $\frac{1}{10}$ (sec) using white light. The dispersion in background densities was found to be less than (0.05) for the photographs used to construct this curve. The (D_I) data points correspond to measurements made at the center of the laser beam image, produced by the CO_2 laser operating in the 10 μm region. The (D_B) data refer to an average of 3 background densities, measured at a distance of 20, 30, and 50 mm from the center of the infrared image. The differences between these two values yields the (D_r) points plotted in Fig. 4.

Figure 4 also illustrates (curve *a*) the typical density obtained for this method when using a green visible exposure of 3-sec duration. For such an experiment the infrared and visible exposures are allowed to overlap so as to reduce relaxation effects of the infrared image, such as the type shown in Fig. 1c.

In this type of recording the film (in this case 55 PN Polaroid) is exposed to a gaussian laser spot of central intensity of 0.3 W/cm^2. After a 3–4-sec IR exposure the visible exposure is begun. Both IR and visible exposures are terminated after an additional 3 sec. The intensity of the green exposure is chosen to produce a background density of 0.5 after 3-sec exposure. Upon development, the film is shown to have been desensitized in the regions of IR exposure. Note also that the desensitization effectively reduces the density of the negative to within 0.2 of the fog level. This type of exposure produces the highest contrast in all cases. If a very short visible exposure is used, say of the order of 0.01 sec, the result is very different.

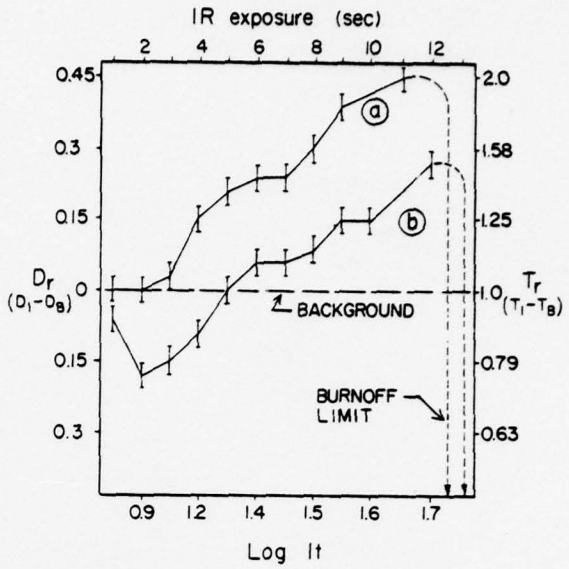


Figure 4. Characteristic curves for IR modification of visible sensitivity, for (*a*) green light, (*b*) white light at IR power density = 0.3 W/cm^2.

In such cases, the desensitization is shown to be replaced by sensitization effects. In such cases the density of the negative IR image is shown to be *higher* than the surrounding background.

Discussion

A number of problems arise when attempts are made to describe a clear and complete mechanism for this effect. Primarily, the fact that the infrared exposure only interferes with, rather than forms, an image is in one sense doubly complicated since uncertainties in the normal photographic processes are masked by unknown infrared effects. There are, however, a number of suggestions which can be offered, suggestions that have already been used to improve photographic response in the infrared.

There are, for example, numerous ways by which latent-image formation can be made less efficient. We are mostly concerned with those which affect the early stages of image formation since no infrared effects are observed for previously exposed emulsions. They include:

(1) Changes in the absorption coefficient of silver halides with temperature.
(2) Loss of photoelectrons
  (a) loss to water
  (b) loss to oxygen and other electron acceptors
(3) Loss of silver
  (a) reactions with holes
  (b) thermal dissociation
  (c) reaction with other agents

Of these, perhaps the most interesting to use are 1, 2(*a*), and 3(*b*). It is well documented that for many emulsion types sensitivity decreases to some extent with elevated temperature.[3–5] Presumably, this effect is partly caused by thermal ejection of an electron (followed by a silver ion) from an unstable latent image center. It is well known that developability is related to latent center size. Removal of even a single $Ag^+ - e^-$ pair from a small (3–5 atoms) silver cluster can reduce developability considerably. This is part of the basis for the Herschel effect mechanism, i.e., thermal breakup of an already formed silver aggregate. It is very probable that the temperature rise in an emulsion exposed to infrared laser energy may

be sufficient to block the formation of latent images. This effect should be observed in emulsions which have been exposed to long duration (1 sec) low-intensity visible light.[3,4] This is indeed the case. Figure 4 and its discussion showed that long visible exposures were required for maximum desensitization contrast. Short visible exposures (<0.01 sec) showed, not only a lack of desensitization under most conditions, but actually a rise in sensitivity in the areas of infrared exposure. The key, of course, is to activate or deactivate the emulsion *before* visible exposure, so that the photochemical processes are affected at the electronic and ionic stages prior to image formation.

In addition, mobility of holes and other electron acceptors increases with temperature[4] which suggests that reactions with latent images or capture of thermally ejected electrons might contribute to the desensitizing effects of high infrared exposure. A reaction with latent images and holes finds some support in the fact that if a film is exposed to infrared energy, then visible, then an additional flash of visible light, there is no indication that sub-image centers are left from the first 2 exposures. If thermal ejection were the only mechanism, some sub-image centers should remain behind, thus altering future emulsion sensitivity in those areas exposed to infrared radiation.

Beyond these considerations, there is the fundamental fact that silver halide absorption changes with crystal temperature,[5] both in terms of absolute absorption and peak absorption wavelength. Therefore, by shifting the wavelength of the visible exposure one can expect different photochemical response at different IR exposure levels. Perhaps there are 2 or more competing processes at work which involve the drift mobility of photogenerated species vs. latent-image formation and fading at different temperatures. In any case the technique has proven useful in that it provides a direct, permanent, transparent record of images from IR laser experiments. There is no distortion introduced by copying optics which must, of necessity be placed oblique to the optical axis of indirect displays such as thermal plates. This facilitates wavelength measurements in spectroscopy and other linear measurement experiments. Contrast is good and has recently been improved by the addition of specific chemicals which are used to more precisely couple infrared action to the grain species. Further experiments are planned and will be presented in future papers. These results are presented primarily to report a new and useful method for middle infrared photography using laser sources and to stimulate further research.

Acknowledgments

This work was supported in part by AFOSR Contract No. F44620-72-C-0076. I would like to express appreciation to Dr. T. D. Wilkerson, Department of Fluid Dynamics, University of Maryland, College Park, and to Mr. J. M. Lindsay, Chesapeake Biological Laboratory, Solomons, Md., for extensive assistance with experiments and discussions in support of this paper.

References

1. Korad Division of Hadron Inc., Santa Monica, Calif.
2. Optical Eng. Inc., Santa Rosa, Calif.
3. J. Malinowski, "Latent Image Formation in Silver Halides," *Photogr. Sci. Eng.*, **14:** 112–121 (1970).
4. T. A. Babcock, W. C. Lewis, and T. H. James, "The Effect of Temperature Upon Photographic Sensitivity for Exposures in Room Air, Vacuum, and Dry Oxygen," *Photogr. Sci. Eng.*, **15:** 297–303 (1971).
5. J. H. Webb, "The Effect of Temperature Upon Reciprocity Law Failure in Photographic Exposure," *J. Opt. Soc. Am.*, **25:** 4–23 (1934).

Versar inc.

T. D. Wilkerson, G. F. Frazier and J. M. Lindsay
Proceedings of DOD Laser Technology Conference
West Point, N.Y. (June 1976)

NEW METHOD FOR IR LASER PHOTOGRAPHY (U)[†#]

T.D. Wilkerson,[**] G.F. Frazier and J.M. Lindsay[††]
Versar Inc., 6621 Electronic Drive, Springfield, Va.

SUMMARY

(Unclassified)

Infrared laser beam patterns can now be photographed directly on conventional silver halide films even though the wavelengths (5, 10 μm) lie well beyond what is ordinarily considered "the photographic infrared". The technique employs sensitization and desensitization of films to visible light as a result of pre-exposure to the infrared radiation. Different photographic regimes exist depending on infrared intensity and length of exposure, and wavelength of the visible light. The range of IR power densities photographed so far is roughly 0.2 - 200 w/cm^2, for IR exposure times of about 2 - 0.02 seconds, respectively. Polaroid emulsions prove to be very convenient, particularly the 55 P/N film; while the effect is seen with all films we have used.

By varying infrared exposure, one can obtain photographic densities which are more or less than the background density due to the visible light alone. IR isophotes within a complex image pattern are therefore visualized as neutral zones between light and dark areas which received less or more IR exposure. The intensity represented by an isophotometric contour can be chosen by changing visible light color and exposure.

On the basis of sensitivity, dynamic range and resolving power, the method is more useful than "image plate" photography (which requires taking a picture of a picture) and "footprint paper". With Polacolor emulsions, photographs have been taken at power density levels corresponding to a 1 mm^2 beam

---

Research supported by AFOSR Contract No. F44620-72-C-0076.

† Patent applied for (G.F. Frazier)
Published article: *Applied Optics* (June, 1976).

** Permanent address: IPSAT, University of Maryland, College Park, Md. 20742
†† Permanent address: Chesapeake Biological Lab, Solomons, Md. 20668

spot of a 1 mw IR laser. The sensitivity and simplicity of the process open up important laser applications such as the recording of dispersed IR spectra and visualizing the motion and far field patterns of laser beams in the atmosphere.

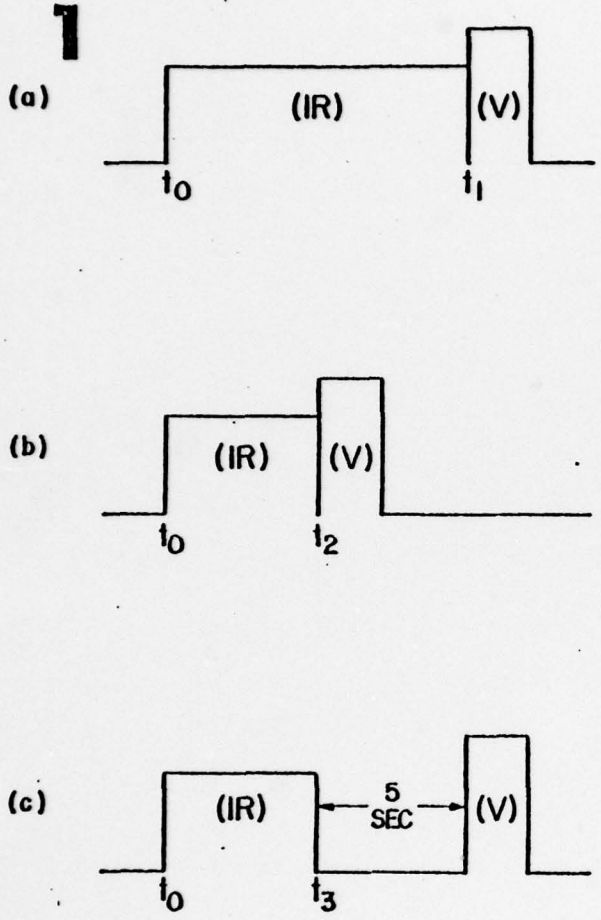
In addition to such applications, we are currently probing the basic mechanisms of the IR influence on latent image formation by the post-exposure, visible flash. Attention centers on changes in the mobility and combination rates of photoelectrons and holes with changing emulsion temperature. We are also considering dye-electron transfers, enhanced by IR exposure. Early results from these lines of study have shown that both relative sensitivity and dynamic range can be improved through carefully chosen exposure parameters. The method is presently useful for low power laser imaging but needs improving to extend sensitivity to very low power applications (1-10 mw/cm^2).

Together with laser imaging applications silver halide chemistry may be studied, especially in the areas of lattice effects due to temperature. Since infrared interaction can be easily controlled, the method provides an ideal medium for determining image relaxation rates, rates of hole recombination and solarization effects at elevated temperature. These preliminary results are encouraging since we have used only "off the shelf" commercial films and large improvements in image quality might therefore be obtained by optimization, through research, of those emulsion qualities which are most suited to infrared recording.

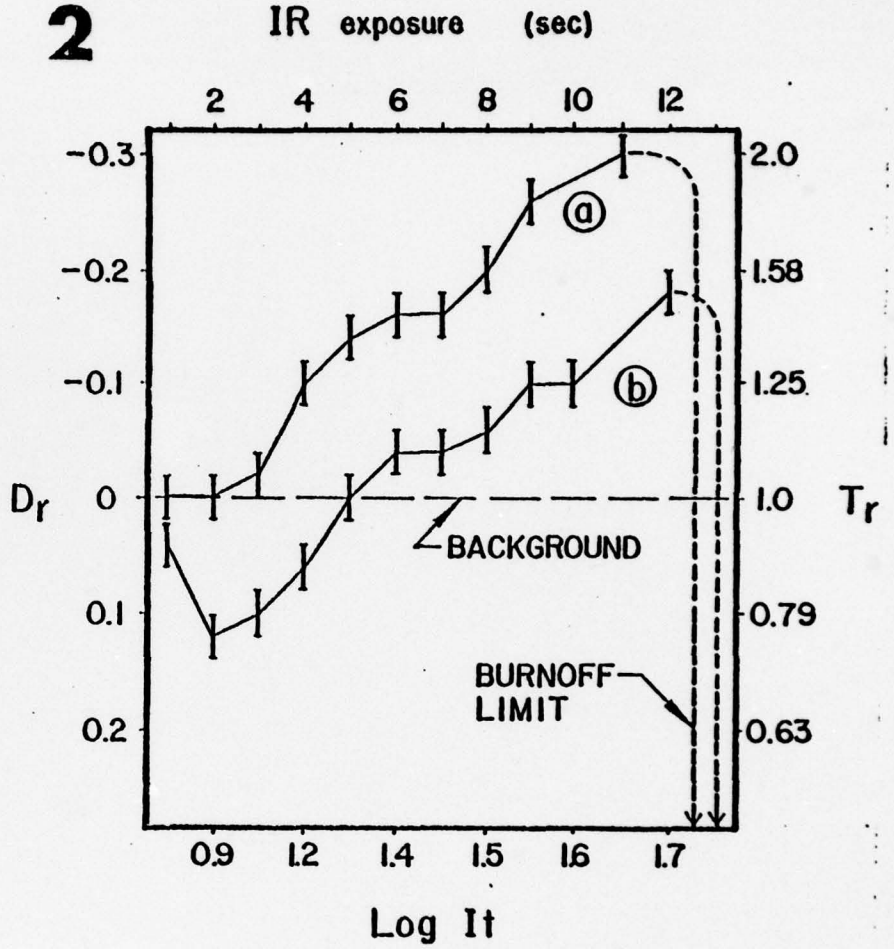
REFERENCES

1. Korad Division of Hadron, Inc., Santa Monica, Ca.
2. Optical Eng. Inc., Santa Rosa, Ca.
3. J. Malinowski, Photogr. Sci. Eng., 14, 112 (1970).
4. T. A. Babcock, W. C. Lewis, P. A. McCue, and T. H. James, Photogr. Sci. Eng., 16, 104 (1972).
5. F. C. Brown and K. Kobayashi, J. Phys. Chem. Solids, 8, 300 (1959).

1


(a)
(IR)
(V)
t_0
t_1
(b)
(IR)
(V)
t_0
t_2
(c)
(IR)
5 SEC
(V)
t_0
t_3

2


IR exposure (sec)
2
4
6
8
10
12
−0.3
−0.2
−0.1
0
0.1
0.2
D_r
2.0
1.58
1.25
1.0
0.79
0.63
T_r
ⓐ
ⓑ
BACKGROUND
BURNOFF LIMIT
0.9
1.2
1.4
1.5
1.6
1.7
Log It

NRL Memorandum Report 3430

Proceedings on a Workshop on Remote Sensing of the Marine Boundary Layer

Vail, Colorado

9–11 August 1976

LOTHAR H. RUHNKE,
Editor

Atmospheric Physics Branch
Ocean Sciences Division

June 1977

NAVAL RESEARCH LABORATORY
Washington, D.C.

Distribution limited to U.S. Government Agencies only; test and evaluation June 1977. Other requests for this document must be referred to the Commanding Officer, Naval Research Laboratory, Washington, D.C. 20375.

INFRARED REFRACTIVE INDEX*

by G. Frazier and T.D. Wilkerson
Versar Inc.
6621 Electronic Dr.
Springfield, Virginia 22151

This paper describes further work on infrared laser photography and progress towards accurate, line-by-line measurements of gaseous index of refraction at IR laser lines. We also note that refractive index signatures for aerosols are sufficiently strong that IR differential absorption lidar systems may be adversely affected unless a thorough line-by-line study is made of laser backscatter.

Figure 1 illustrates a further development in the IR photographic method recently described.[1] The same IR laser beam spot is photographed in all three cases, by visible post-exposure of the Polaroid 55-PN negative. In each case, infrared exposure was three seconds at a constant power density of 0.3 w/cm^2. The varying parameter is the intensity and duration of the visible exposure. From left to right, visible exposure was .004, .15 and 1 sec. The density within the areas of infrared exposure are dependent upon the ratio of IR/VIS photons illuminating the grain.

The photograph shows that the crossover from desensitization to sensitization can be chosen for different IR intensity levels, depending on the visible exposure time. This display capability for bringing out one or more IR-isophotometric contours is very useful in depicting the intensity distribution within a laser beam pattern. We have extended the IR power density range to 10 - 100 w/cm^2, and are designing a cinematographic version for framing rates up to ~50 sec-1.

That this IR recording method is dry, inexpensive and uses simple photographic materials makes it very attractive for operational use. Testing and verification of electro-optic system performance can be made simple with this method.

*Research supported by AFOSR Contract No. F44620-72-C-0076

[1] G. Frazier, T.D. Wilkerson and J.M. Lindsay, Applied Optics, 15, 1350 (1976).

The above process was discovered during Air Force-sponsored research on infrared schlieren systems and other IR extensions of flow visualization methods in visible light. Selective schlieren sensitivity to various molecules is anticipated by matching the probe laser lines to the refractive index extremes near absorption lines (anomalous dispersion). Optimization of this technique calls for line-by-line measurements of the refractive index for various gases. The results will also bear directly on laser beam propagation in the atmosphere. Two levels of measurement are described here as part of our overall program which is aimed toward (n-1) results having an accuracy of $1:10^8$ or better.

Figure 2 shows the first experimental arrangement, where the test gas (e.g., 3% O_3 in O_2) was confined in a hollow prism having NaCl windows. Angular deflections are measured as a function of laser (CO_2) wavelength, yielding the index of refraction, $n(\lambda)$, in the ozone band near 9.4 μ.

Figure 3 shows somewhat averaged-out measurements of $n(\lambda)$ compared to the ozone extinction[2] in the 9.4 μ band. The wavelength averaging is due to several emission lines in the CO_2 laser which had not been carefully selected between in this early work. One sees the maximum index near the 9.6 μ absorption minimum. This is clearly the best wavelength region for IR schlieren studies of O_3, while a long-path laser system in an ozone-rich environment would be more affected at 9.6 μ by atmospheric schlieren, than at 9.2 or 10.6 μ.

Figure 4 shows the next stage of measurements using a Michelson interferometer whose fringes are counted as the gas of interest is cycled into and out of the cell. Single laser selection is achieved with an intracavity etalon. Fringe-fractions of order 1/50 are reliably observable if one uses the indicated gain-stabilizing system to automatically compensate for variations in laser output power. This particular system does not automatically compensate for IR absorption in the interferometer's gas cell.

Results are shown in Figure 5 for the refractive index of N_2 as measured line-by-line in the CO_2 laser region. Thirty-six observations go into each point, so that the accuracy can be made $\sim 1:10^7$. The "calculated value" of (n-1) for nitrogen in this region is taken from a Sellmeir equation

[2]Courtesy Dr. John Gaugliardo, EPA, Las Vegas (Private communication, 1975).

given by Peck[3], and no inconsistency appears as yet. This work continues with other gases, and with control systems that remove the effects of absorption in the gas cell. Thus, we can now measure $(n-1)^{IR}$ to about $1:10^8$ and make a line-by-line assessment of the susceptibility of any given laser line to atmospheric density gradients.

Our interest in refractive effects extends now to aerosols, since their IR index signatures are strong enough to influence backscatter differentially in wavelength. This may compromise near-IR lidar performance for remote sensing of H_2O and other species. Examples of the wavelength sensitivity of backscatter by aerosols have been given by Pollack and Colburn[4] and by Shettle[5] at this meeting, and proposals have been made to use this effect for aerosol composition determinations.

In view of the complexity of the relationships between backscatter, aerosol refractive index, particle shape and size distinction, we believe that a major program of diverse measurements on backscatter and extinction needs to be undertaken for near-IR lidar systems. Our proposal for such a program is currently in preparation. The effects of gaseous refractive index will also be considered in this work, and use will be made of the IR photographic process in displaying beam scatter and beam spread by aerosols.

---

[3] E. Peck, Dispersion of Nitrogen, Appl. Optics, 10, 107 (1962).
[4] J. Pollack and D.S. Colburn, Proc. VII Lidar Conference, SRI (Nov. 1975).
[5] Shettle, paper, Session I: The Marine Atmospheric Environment

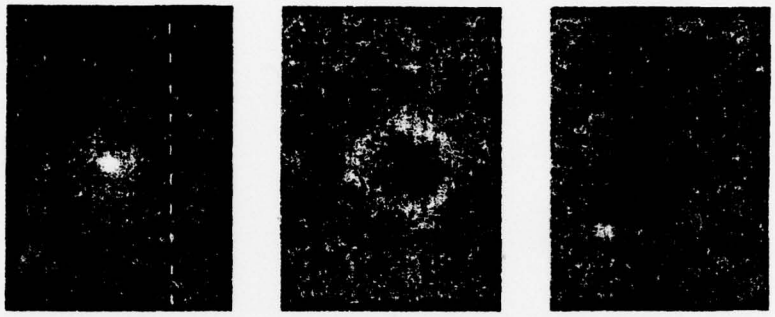


Fig. 1.

A Mosaic of Three Infrared Laser Beam Patterns

From left to right: sensitization of the film in the area of IR exposure, sensitization ring with central desensitized region, and desensitization. In each photograph, IR intensity and exposure is constant but the visible post exposure intensity is decreasing, left to right.

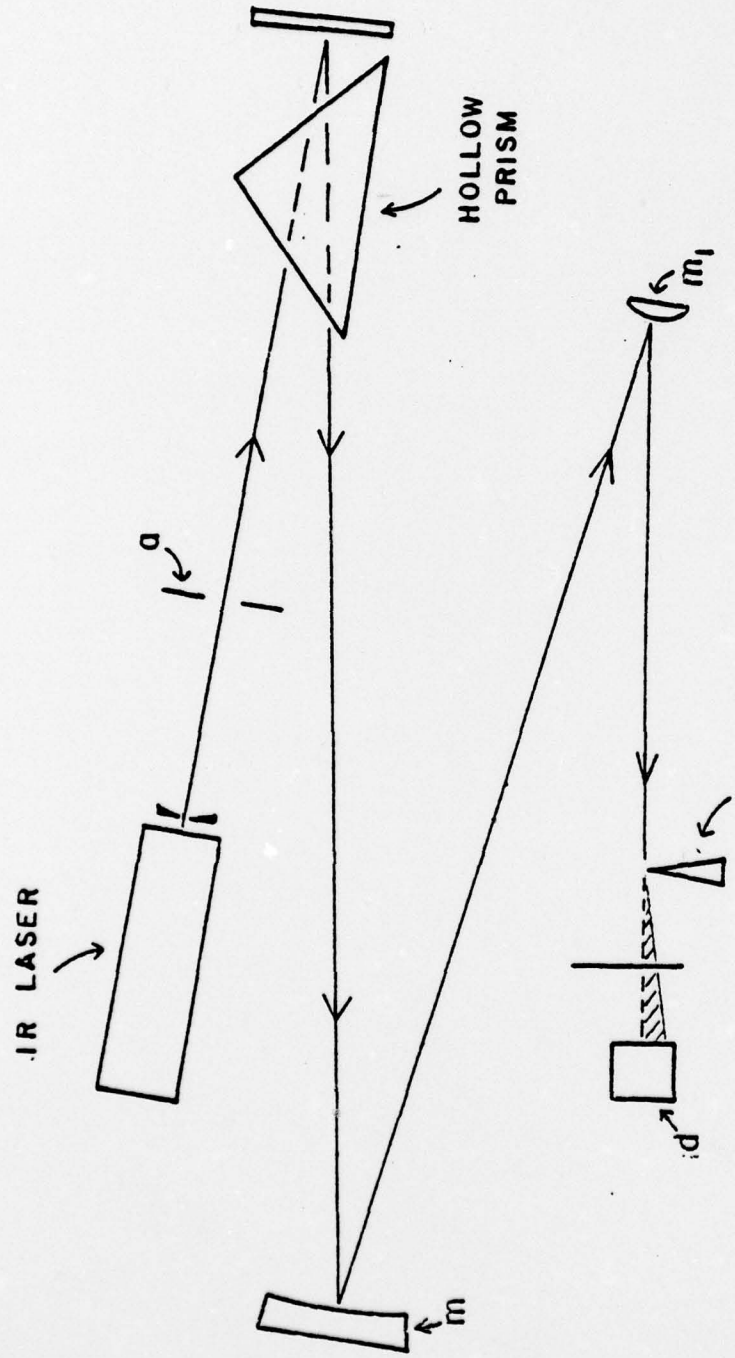


Fig. 2.

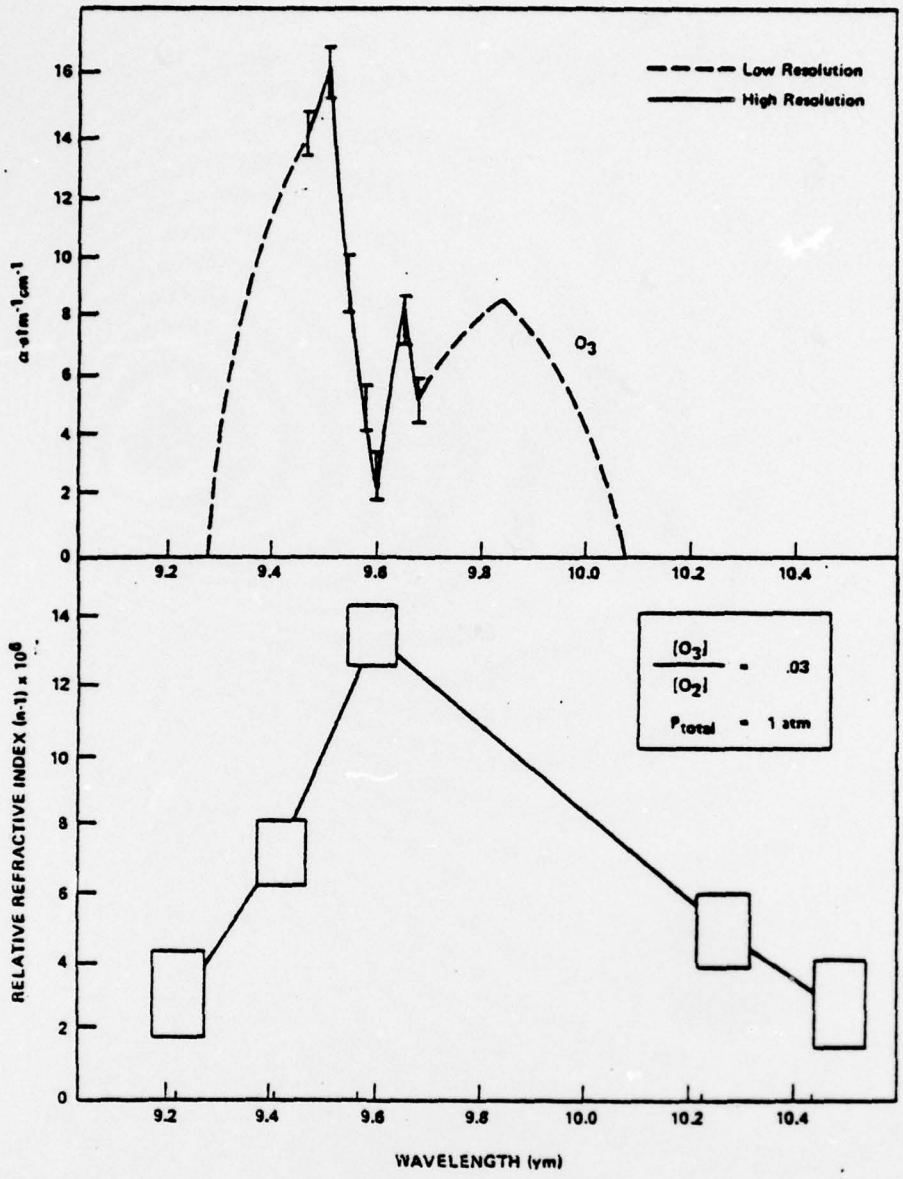

Low Resolution
High Resolution
O_3
α (atm^{-1}cm^{-1})
RELATIVE REFRACTIVE INDEX (n-1) x 10^6
$\frac{[O_3]}{[O_2]}$ = .03
P_{total} = 1 atm
WAVELENGTH (μm)

Fig. 3.

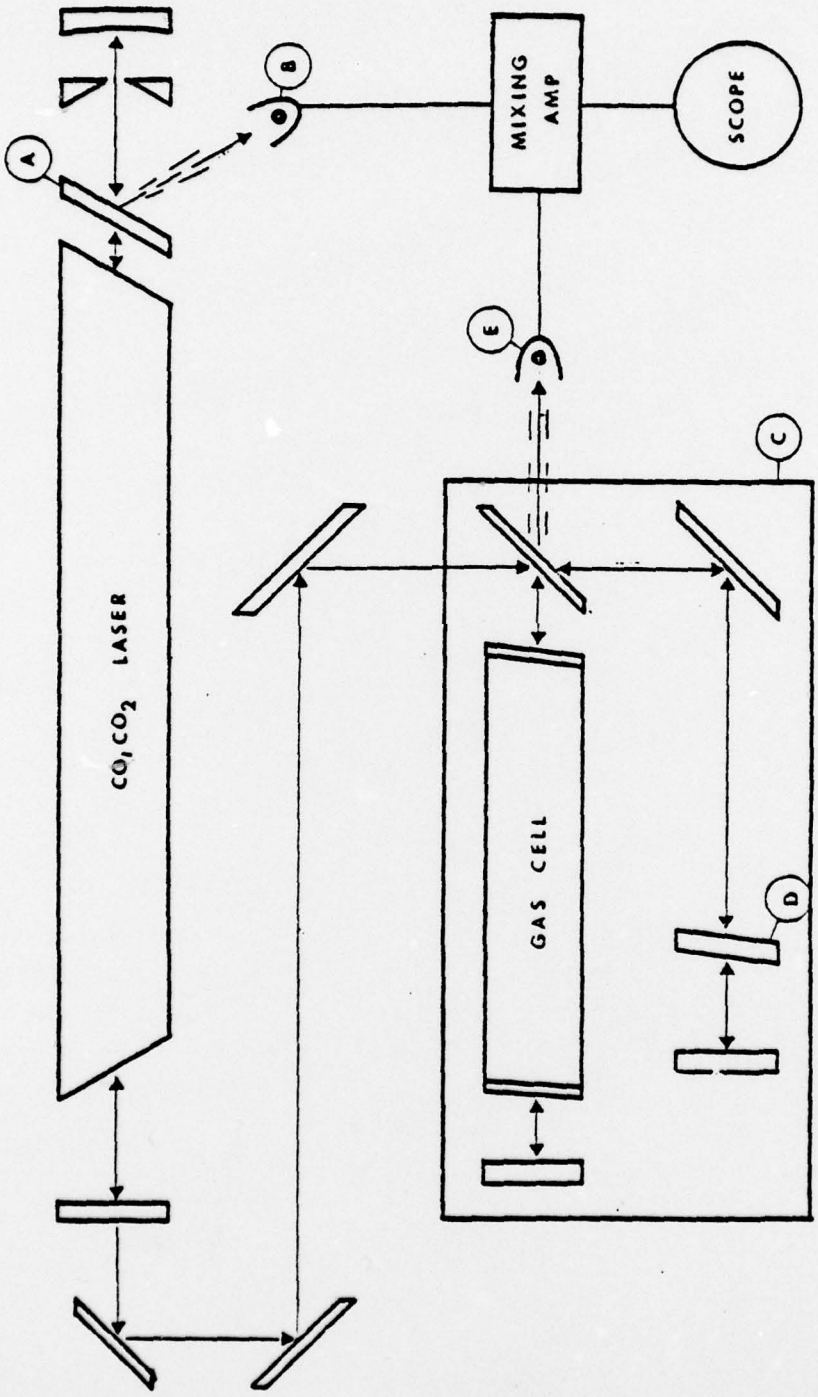


Fig. 4.

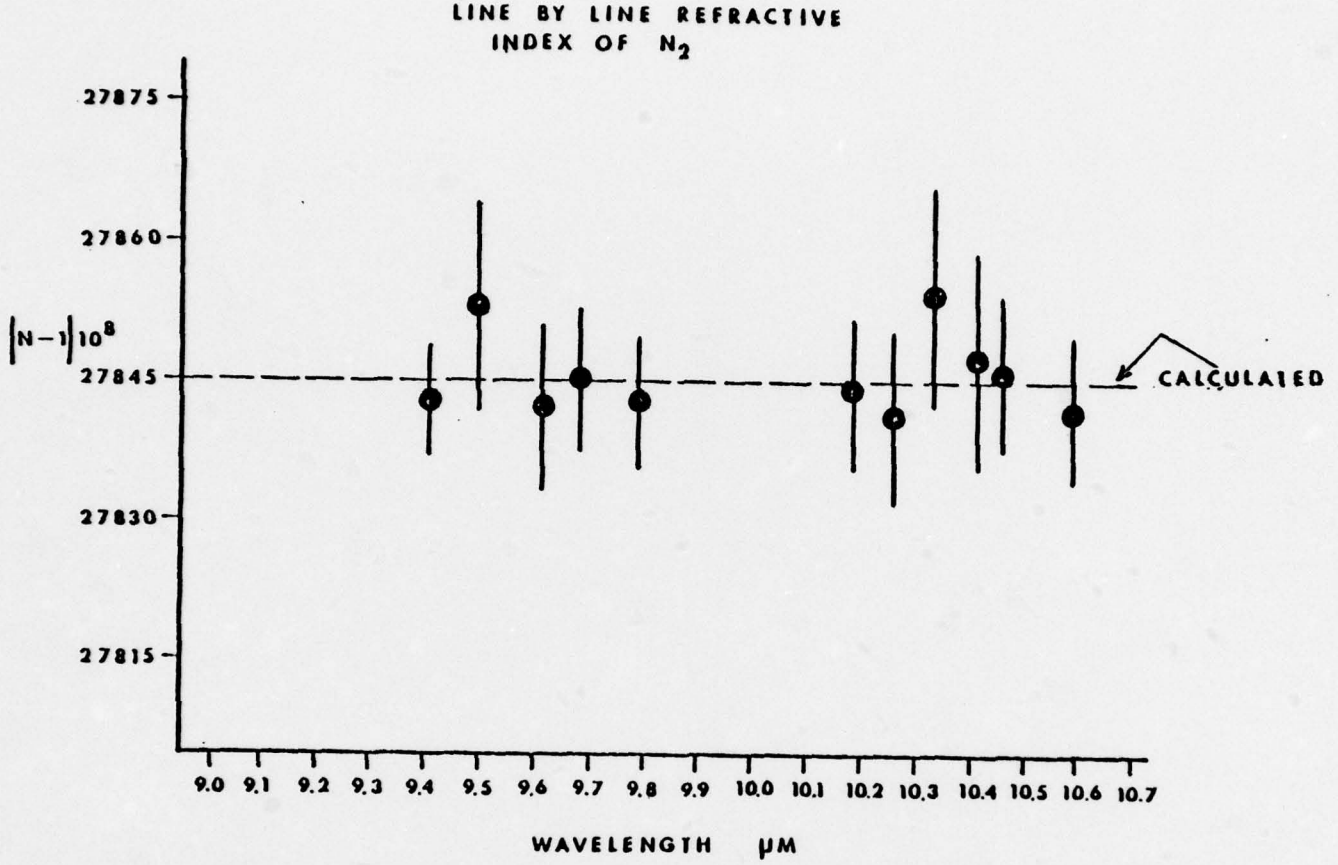

LINE BY LINE REFRACTIVE
INDEX OF N_2
27875
27860
$|N-1|10^8$
27845
27830
27815
CALCULATED
9.0 9.1 9.2 9.3 9.4 9.5 9.6 9.7 9.8 9.9 10.0 10.1 10.2 10.3 10.4 10.5 10.6 10.7
WAVELENGTH μM

Fig. 5.